Synthesis and Characterization of Modified Chitosan-based Novel Superabsorbent hydrogel: Swelling and Dye Adsorption behavior

Akeem Adeyemi Oladipo

Submitted to the
Institute of Graduate Studies and Research
in partial fulfilment of the requirements for the Degree of

Master of Science
in
Chemistry

Eastern Mediterranean University
September 2011
Gazimağusa, North Cyprus

Approval of the Institute of Graduate Studies and Research

Prof. Dr. Elvan Yılmaz

Director

I certify that this thesis satisfies the requirements as a thesis for the degree of Master of Science in Chemistry.

Prof. Dr. Mustafa Halilsoy

Chair, Department of Chemistry

We certify that we have read this thesis and that in our opinion it is fully adequate in scope and quality as a thesis for the degree of Master of Science in Chemistry.

Prof. Dr. Elvan Yilmaz	Asst. Prof. Dr. Mustafa Gazi
Co-supervisor	Supervisor

Examining Committee

1. Asst. Prof. Dr. Fevzi Çakmak Cebeci
2. Assoc. Prof. Dr. Hasan Galip
3. Asst. Prof. Dr. Mustafa Gazi

ABSTRACT

Lately, a wide application of eco-friendly polysaccharide-based hydrogels in waste water treatment has received enormous attention in the literature. Particularly, the development of super swelling chitosan-based materials as versatile and useful adsorbent polymeric agent is an expanding area in the field of adsorption science today. The effluents containing dye materials from the processing industries are washed off into rivers and lakes which can be very harmful to creatures. Low-cost biopolymers and biodegradable adsorbents have been researched to be a good tool to minimize the environmental hazards caused by the industrial effluents by removal of these toxic and carcinogenic dyes from the waste effluents.

In this work, a novel superabsorbent hydrogel was synthesized using water-soluble glycidyl methacrylated *N, O*-(2, 3 dihydroxypropyl) chitosan (DHPC-GMA) and acrylamide (AAm) as reactants. A feasible synthesis was achieved due to the incorporation glycidyl methacrylate (GMA) into the structure of water soluble chitosan, *N, O*-(2, 3 dihydroxypropyl), (DHPC) to form the water soluble chitosan-methacrylated (DHPC-GMA), in a calculated mixture of water-DMSO as solvent and TEMED as catalyst. Thereafter, the DHPC-GMA was copolymerized in potassium persulfate aqueous solution with AAm yielding superabsorbent (DHPC-GMA-g-PAAm) hydrogel. The incorporation of GMA on DHPC molecules was confirmed by FTIR by the presence of a band at 1637cm^{-1} indicative of C=C stretching frequency and strong broad band in the region 1711-1641 cm^{-1} in DHPC-GMA-g-PAAm hydrogel spectrum attributed to the overlap of the C=O stretching bands of esters of

DHPC-GMA, primary amides and N-H deformation of primary amide from AAm indicating copolymerization of DHPC-GMA with AAm.

The maximum grafting percentages (%G) and grafting efficiency (%E) for hydrogel sample B, C and D with varying monomer (AAm) concentration are %G; 150, 304, 995 and %E; 49.8, 60.8, 99.5 respectively. The synthesized hydrogel shows super swelling ability with swelling percentage of about 1900% and the swelling kinetic fits well with second-order- kinetic model.

A batch system was applied to study the adsorption behavior of Reactive blue 2 (RB2), Erichrome Black T (EBT) and mixture of both dyes in aqueous solution by the DHPC-GMA-g-AAm hydrogel. The adsorption capacities were 38.02mg/g EBT and 32.73mg/g RB2 for sample D with highest grafting percentage and 12.79mg/g EBT and 58.14mg/g RB2 for sample B with the lowest grafting percentage. The adsorption of both single and mixture of dyes onto the hydrogel fit with the second-order kinetic model and the kinetic data is in good agreement with the experimental data having high correlation coefficients (R^2 = 0.999). The competitive adsorption favored the dye EBT in the mixture solution and the percentage removal of EBT reaches 63.4% at 48 hr contact time which is larger than 36.5% of RB2 in same solution.

Keywords: Superabsorbent hydrogel, characterization, erichrome black T, reactive blue 2, competitive dye adsorption, water-soluble chitosan

ÖZ

Son zamanlarda, doğa dostu polisakkarit bazlı hidrojellerin biyomedikal alanlarda ve atık su iyleşmelerindeki geniş uygulamaları literatürde büyük önem görmektedir. Özellikle, çok yönlü ve kullanışlı absorban polimerik ajan olarak, süper şişen kitosan bazlı malzemelerin geliştirilmesi, bugünkü adsorpsiyon bilim alanında gelişen bir alandır. Endüstriyel proseslerden çıkan boya içerikli malzeme atıkların nehir ve göllere atılımı calılar için oldukca zararlıdır. Endüstriyel atıkların sebep olduğu bu toksik ve kanserojenik boyaların giderimi için düşük maliyetli biyopolimerler ve biyoparçalanabilir adsorbentler iyi birer araçtırlar.

Bu çalışmada, kimyasal olarak modifiye edilmiş, suda çözülebilen glisidil metakrilatlanmış *N, O*-(2, 3 dihydroksipropil) kitosan (DHPC-GMA) ile akrilamid (AAm) reaktifleri kullanılarak, yeni bir süperabsorbent hidrojel sentezlenmiştir. Su-DMSO karışımı ve TEMED katalizörü varlığında glisidil metakrilatın (GMA), suda çözülebilen *N, O*-(2, 3 dihydroksipropil) kitosan (DHPC) ile birleşimi ile suda çözülebilen metakrilatlanmış kitosan (DHPC-GMA) formunun sentezi başarılmıştır. Daha sona, potasiyum persülfat çözeltisinde DHPC-GMA ile AAm kopolimerleştilerek süperabsorban (DHPC-GMA-g-PAAm) hidrojel ürünü elde edildi.

DHPC molekülüne GMA'nın eklenmesi FTIR spektroskopideki 1637cm^{-1} deki bandın varlığı C=C gerilme frekansını göstermesiyle onaylanırken, DHPC-GMA-g-PAAm hidrojel spektrumunda 1711-1641 cm^{-1} bölgesindeki geniş güçlü bandın DHPC-GMA'nın ester grubunun C=O gerilme bandı, birincil amid ve AAm'in

birincil amidinin N-H deformasyonu ile örtüşmesi DHPC-GMA ile AAm kopolimerizasyonu göstermektedir.

Çeşitli monomer (AAm) konsantrasyonlu B,C ve D hidrojel örneklerinin, maksimum aşılanma yüzde (%G) ve aşılanma etkinlikleri (%E) sırası ile %G; 150, 304, 995 ve %E; 49.8, 60.8, 99.5'dir. Sentezlenmiş hidrojeller yaklaşık 1900 % şişme yüzdeli süper absorpsiyon yeteneği göstermekte ve kinetik şişmesi ikinci dereceden kinetik modelle örtüşmektedir.

Reaktif mavi 2 (RB2), Erikrom siyah T (EBT) ve her ikisinin karışımının sulu çözeltilerinin DHPC-GMA-g-PAAm hidrojelleri tarafından adsorpsiyon davranış çalışmaları için batch sistemi uygulanmıştır. Yüksek aşılanma yüzdesine sahip D örneğinin adsorpsiyon kapasitesi EBT için 38.02mg/g ve RB2 için 32.73mg/g iken düşük aşılanma yüzdesine sahip D örneğinin adsorpsiyon kapasitesi EBT için 12.79mg/g ve RB2 için 58.14mg/g olarak belirlenmiştir. Hidrojeller üzerinde her iki boyanın tek başlarına ve karışım olarak adsorpsiyonu ikinci dereceden kinetik modele uymakta ve kinetik veriler deneysel verilerle yüksek korelasyon katsayıyla (R^2 = 0.999) örtüşmektedir. Rekabetçi adsorpsiyonda, karışım çözeltisindeki EBT boyası tercih edilmekte ve 48saatlik etkileşim süresinde yüzde giderim %63.4 EBT, % 36.5 RB2 olmaktadır.

Anahtar kelimeler: Süperabsorban h idrojel; karakterizasyon; erikrom siyah T; reaktif mavi 2; suda-çözülür kitosan; rekabetçi boya adsorpsiyonu

ACKNOWLEDGMENTS

I am heartily thankful to my ideal thesis supervisor, Assist. Prof. Dr. Mustafa Gazi, whose sage advice, patient encouragement, guidance and steadfast support from the initial to the final level, aided the writing of this thesis in innumerable ways. One simply could not wish for a better or friendlier supervisor.

I would also like to express my sincere thanks to Prof. Dr. Elvan Yilmaz for her unselfish advice and unfailing support as my co-supervisor and tutor.

I thank my fellow labmates in Eastern Mediterranean University: Zulal and Abdulmuni, for the stimulating discussions and suggestions.

Lastly, I offer my regards to my family, my little “Henrietta” and blessings to all of those who supported me in any respect during the completion of this thesis.

TABLE OF CONTENTS

LIST OF FIGURES

LIST OF TABLES

LIST OF SCHEMES

NOMENCLATURE

a) DHPC : 2, 3-Dihydroxypropyl chitosan

b) GMA : Glycidyl methacrylate

c) DHPC-GMA : Glycidyl methacrylated 2, 3-dihydroxypropyl chitosan

d) DHPC-GMA-g-PAAm : Superabsorbent hydrogel

e) PAAm : Polyacrylamide

f) RB : Reactive blue 2

g) EBT : Erichrome Black T

Chapter 1

INTRODUCTION

Searching for eco-friendly superabsorbent hydrogels is directly linked to the synthesis of bio-materials which can absorb a large amount of water or bio fluids and that can be utilized as absorbents in personal hygiene products, as dye adsorbents from waste water and soil conditional [1,2]. Researchers have contributed largely to find low-cost adsorbents with greater adsorption capacities that can remove dyes from the effluents and recently superabsorbent hydrogels have evoked wide attention for its great ability to remove dyes which can be attributed to its intrinsic features such as high oxygen permeability and less interfacial tension [3].

Superabsorbent hydrogels (SAH) are three dimensional polymer matrices with an appropriate degree of cross linking and differing functional groups such as hydroxyl, amine, which have ability to absorb and retain voluminous amount of water, bio-fluid or trap dyes from aqueous solution [4]. This property of SAH is the reason behind its varied applications ranging from pharmaceutical matrices, especially for drug delivery systems, materials for agricultural nutrients and food additives [5]. Chitosan based hydrogels were prepared and were found to have various applications due to their structural make up and intrinsic characteristics [19]. Recently, much interest has been shown in the synthesis and modification of chitosan based superabsorbent hydrogels due to their excellent characteristics and good numbers of researchers have found wide applications of chitosan-based SAH as dye removal,

drug delivery system and as agricultural water reservoirs [17]. The removal of dyes from waste waters has created paramount attention because of two main reasons; (1) even traces of dyes in water changes the color and (2) create environmental pollution affecting living being [17]. The pollution potential of dyes in waste water has been triggered by the concern over their carcinogenicity as most dyes are produced from carcinogens which might be transformed as a result of microbial metabolism [44].

Also azo- and nitro- derivative dyes can regenerate parent toxic amines when reduced in sediments or intestinal region [44]. Research has shown that the most used dyes in industries are the reactive, basic and azo dyes [45] and the amount of dye washed into the water bodies is approximated to be 15-65% for reactive dyes, 1-8% for basic dyes and 10-30% for azo dyes [46]. It is very fundamental to remove these dyes as their existence within the storage tank is very high [45]. Reactive Blue 2 one of the reactive dyes has three Sulphonic units, amino units and chlorotriazine group are present on the reactive blue 2 structure, and the chlorotriazine unit is responsible for the reactions with the functional groups of the chitosan-based superabsorbent hydrogels [47].

Erichrome Black T is an important class of azo dye, having azo bond and sulphonic group on its structure and is widely used in many industries for coloring their products [48]. A lot of work has been done on the removal of dyes by variety of chitosan-based hydrogels and these give adsorption capacities within the range 25-2500mg/g [49].

This research is aimed at the synthesis of a water-soluble chitosan-based novel superabsorbent hydrogel and to characterize the resulting hydrogel. The synthesized

hydrogel is expected to have good swelling properties and ability to remove trace amount of dyes in contaminated waste water. In this study, the swelling behavior of the hydrogel and comparative removal of reactive blue 2 and Erichrome black T by the synthesized hydrogel were investigated.

1.1 History of Superabsorbent hydrogels

The earlier water-absorbent hydrogel was produced in early 1938; divinylbenzene and acrylic acid (AA) were polymerised in an aqueous medium [6]. The earlier member of hydrogels comes into existence in the late 1950s which were based mainly on hydroxyl alkyl methacrylate and closely-linked monomers with swelling capacity up to 45%. They were used in producing contact lenses which was a great revolution in ophthalmology [7]. The first commercial SAH was produced in the united state department of agriculture through alkaline hydrolysis starch-graft-polyacrylonitrile in the early 1960s [8].

1.2 Properties of Superabsorbent Hydrogel

Superabsorbent hydrogel is polymeric material, which has ability to absorb and retain water or other bio-fluids in aqueous or biological environment [9]. The hydrophilic chains of the SAH do not dissolve into aqueous phase due to the fact that the polymeric chains are linked to one another by cross linkers [10]. SAH has the ability to trap ionic dyes from wastewaters due to the presence of ionic functional units on its backbone. SAH is an ideal biomaterial in drug delivery due to its ability to swell and retain the fluid in biological region. The following reaction variables affect the final properties of SAH [15].

i. Cross linker concentration and type
ii. Polymerization temperature

iii. Monomer type and concentration

iv. Post-treatment such as surface cross linking

Table 1: Superabsorbent hydrogel properties are affected by the following factors [16].

Variation in synthetic factor	*Absorption capacity*	*Absorption rate*	*Gel strength*
Increase in initiator concentration	↑	↓	↓
Increase in Monomer concentration	↓	↑	↓
Increase in cross linker concentration	↓	↓	↑
Surface cross linking	↓	↔	↑
Increase in reaction temperature	↑	↓	↓

↑ = increasing ↓ = decreasing ↔ = varied

1.3 Preparation methods of Superabsorbent hydrogels

Superabsorbent hydrogels are three-dimensional polymeric network and its crosslink's need to be available so as to prevent disintegration of the chain in aqueous environment. In most cases the polymeric network structure of SAH has to breakdown into harmless non-hazardous product and to ensure good biocompatibility of the gel. Variety of chemical and physical cross linking techniques have been designed for the development of biocompatible hydrogel.

Most of the SAHs are synthesized from synthetic polymeric materials nowadays [13] but global decision supports the replacement of the synthetic material with more economical and "environmental friendly" substitutes [14]. The SAH can be

effectively prepared from carbohydrate polymers as they are readily available and cheap to source.

Generally, the natural-based SAH preparation is held into two categories; (i) Graft polymerization (ii) cross-linking reaction. Polysaccharides undergo reactions with initiators in one of the two ways below;

First, the OHs on the saccharide units and the initiator interact to form redox pair-based complexes. These complexes are subsequently dissociated to produce carbon radicals on the saccharide substrate via homogenous cleavage of the saccharide C-C bonds. These free radicals initiate the graft polymerization of the vinyl monomers and cross-linker on the substrate. Second, an initiator such as persulphate may abstract hydrogen radicals from the OHs of the polysaccharide backbone.

1.4 Classification of Superabsorbent hydrogel

Superabsorbent hydrogel can be grouped into four classes based on (i) availability and non-availability of charges on the cross linked chains or nature of the side groups (Amphoteric, Ionic) (ii) on method of preparations (copolymer, homo-polymer) (iii) physical structure (Amorphous, Semi-crystalline) (iv) origin (Synthetic, Natural). An important class of SAH is the stimuli responsive gels [11]. These superabsorbent hydrogels show swelling behavior which depends on their physical environment and this gel can swell or deswell due to variations in ionic strength, temperature and pH [12]. This unique property allows the SAH for usage as biosensors and bio-active delivery devices [11].

1.4.1. Chitosan-based Materials

A natural polymeric carbohydrate structures in which its repeating units are joined together by a covalently glycosidic bonds are referred to as polysaccharides. These macromolecules are readily available biomaterials and some of the most important polysaccharides are cellulose, chitin, pectin, starch and natural gums. In recent years, scientists turned their attention to a polysaccharide namely chitosan an amino derivative of chitin.

The practical application of chitosan has been limited to the raw chitosan but chemical modification on the chitosan is a great breakthrough in its utilization and this has been reported to lead to the development of new materials. Chitosan has an uncompromising advantage over other polysaccharides due to the fact that its functional groups can be easily modified [19].

Lately, workers have shown varying interest in the synthesis and modification of chitosan based superabsorbent hydrogels due to their excellent characteristics and good numbers of researchers have found wide applications of chitosan-based SAH such as dye removal, drug delivery carriers and agricultural water reservoirs [17]. The reactive functional groups on this biopolymer can be used to alter its properties chemically under stringent reaction environment. Great numbers of workers have reported the excellent biocompatibility of chitosan and this has triggered the voluminous use of chitosan in medical field and as sorbent for waste water treatment. The deacetylated derivative of chitin is highly efficient for interacting with anionic solutes and dyes in solutions due to the availability of amine on its backbone [18].

Chitosan is a natural cationic amino polysaccharide which breaks down to harmless amino sugar product and completely absorbed by human body [20]. Chitosan has been used for variety of functional materials including biomaterials; however its applications are limited in biological industry due to its high viscosity [21]. Recently, investigation on water-soluble chitosan shows it has health benefits such as anti-tumoral and as immunity regulation agent [22].

1.1.1.1 Cross linking strategies of chitosan-based hydrogels

Chitosan-based hydrogels are cross linked higher molecular networks that have the ability to swell in wide range of bio-fluids or water and these materials have become potential bio-carriers of active components in their swollen state [23-27].

1.1.1.2 Applications of chitosan-based Superabsorbent hydrogels

In case where greater bioadhesivity and higher adsorption capacity are required, chitosan-based materials are the most suitable superabsorbent hydrogel material because of their low cost, the large availability and the responsiveness of the modified chitosan to variation of external stimuli.

Chitosan offers several advantages as biosorbent for removing dyes from solutions. Besides being naturally available and non-toxic, chitosan possess intrinsic properties which make it an efficient dye adsorbent. The factors that made the utilization of chitosan global are:

i. Chitosan-based materials are cheap and naturally available. Wastes from aquatic body are good sources of chitosan because such waste is abundantly available in large quantities and economically low cost.

ii. Researchers have reported that chitosan shows great absorbent capacities and also poses an outstanding greater selectivity in cleaning range of solutions.

iii. Lastly, the versatility of chitosan due to the development of new complexing material makes chitosan an ideal material for removing dyes.

Table 2: Applications of Chitosan-based SAH

Chemical industry	● Personal hygiene products
	● Metal chelation
Pharmaceutical industry	● Controlled drug delivery agent
	● Wound dressings and bulking agents
Environmental	● water treatment (Dye removal)
Agriculture	● Water reservoirs
	● Soil treatment

1.4.1.2.1 Chitosan-based SAH as a biosorbent for dye removal

Dye is one of the organic materials which find wide use in textile and paper industries for dyeing and finishing and these dyes are washed off in water waste and they exist as undesirable material in the environment since not all of the dye molecules could bind with the material during the production steps. The variety of use of synthetic dyes in many fields posed harmful effects on humans and this can be disastrous. The removal of color from contaminated water is a great environmental problem due to the difficulties and expense that is involved when conventional methods are used. Recently, different methods have been reported for cleaning dye-containing waste waters which includes extraction, ion-exchange, membrane filtration, photo-catalysis degradation, absorption and adsorption [28-30]. Among them, adsorption on chitosan-based SAH has been identified as a favourable technique due to its bioadhesivity properties, cheap sources and availability [29].

Chapter 2

EXPERIMENTAL

2.1 Materials

A low viscosity chitosan flake (Fluka) of molar mass 1.5×10^5 with 100 mPa.s and 85% degree of deacetylation was used as the starting material. Acrylamide (Aldrich), Sodium hydroxide (Aldrich), hydrochloric acid 37% (Riedel-de Haen), Potassium persulfate (KPS, Merck), *N*,*N*,*N*′,*N*′-Tetramethylethylenediamine 99.5% (TEMED, Aldrich), Dimethyl sulfoxide (DMSO, Merck), Glycidol (Fluka), Reactive Blue 2 60%(Aldrich), Erichrome Schwarz T (Merck), Acetone (Aklar) and glycidyl methacrylate (GMA, Aldrich) were used as supplied. Analytical grade of other chemicals were used.

2.2 Methods

2.2.1 Preparation of Water-soluble chitosan derivatives

Water-soluble chitosan derivative was prepared in two different steps according to the literature [40]. The steps of synthesis are given in Scheme 1. According to the literature [40], water-soluble chitosans are prepared by the reaction of chitosan with epoxides and glycidol. Based on the experimental conditions of the epoxide the reaction might occur chiefly at the hydroxyl or amino group, to yield N-hydroxyalkyl or O-hydroxyalkyl chitosans or a mixture of both (scheme 1). The ratio of O/N-substitution is determined by the nature of catalyst used (NaOH or HCl) and the reaction conditions [50]. N-hydroxypropylation is obtained without catalyst, while

under acid catalysis N- product will be achieved and some O-alkylation products might be present. Under basic media O-alkylation is preferred with a greater tendency to yield oligomers at higher temperature greater than 40^{o}C [50].

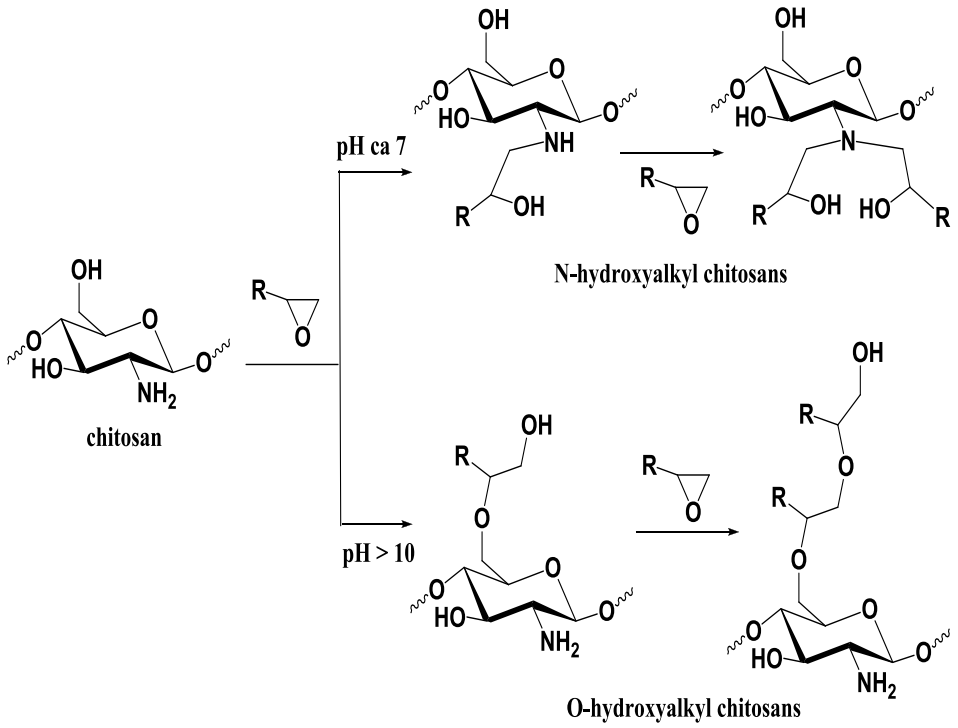

Scheme 1: Reactions of chitosan with epoxide. [R= H, - $(CH_2)_n$-CH_3, n= 0 or 1]

2.2.1.1 Synthesis of N, O-(2, 3 dihydroxypropyl) chitosan

2, 3-Dihydroxypropyl chitosan (DHPC) was prepared in two main steps; the first step was the synthesis of *N*-(DHPC) under neutral pH. 5mL 3-hydroxypropylene oxide added to chitosan mixture (2.5g) in water (25mL) in a flask and the mixture was stirred continuously under heat at 90°C for 1day. It was followed by addition of excess 3-hydroxypropylene oxide which was stirred continuously to yield *N*-(DHPC). *N*, *O*-(2, 3 dihydroxypropyl) chitosan was synthesized in the second step under alkali condition. 5mL NaOH (1.5M) was added to the resulting mixture in the first step and put into a refrigerator at -18°C for alkalization. 5mL 3-

hydroxypropylene oxide was added to the alkali chitosan at 90°C with continuous stirring for one night. 1.1 (v/v) HCl was added to the reaction mixture so as to adjust it to pH 7.0, filtered and the product obtained was washed continuously by acetone and then dried at 60°C in oven for 2days [51].

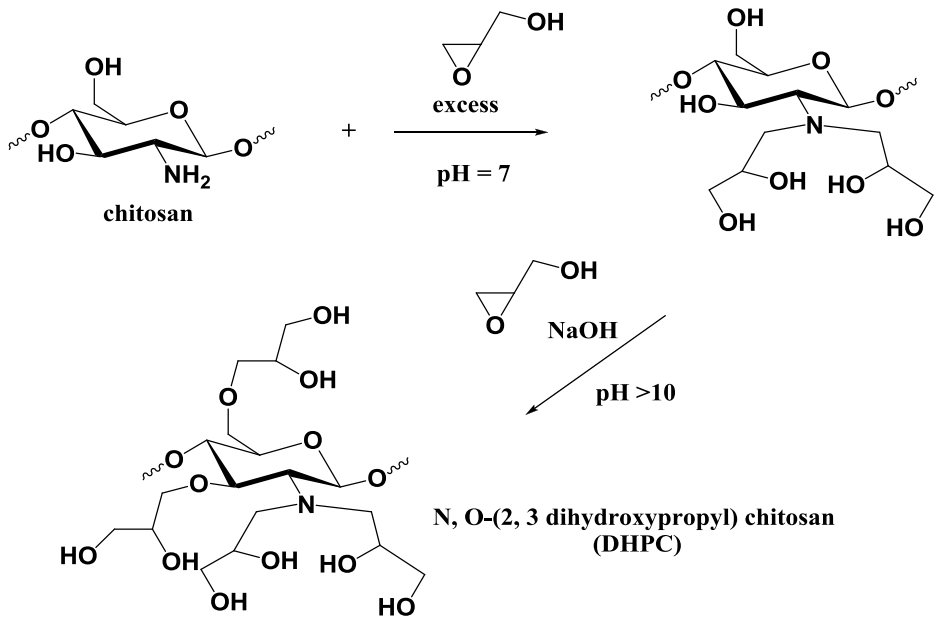

Scheme 2: Outline of the synthesis of *N, O*-(2, 3 dihydroxypropyl) chitosan

2.2.1.2 Synthesis of GMA modified N, O-(2, 3 dihydroxypropyl) chitosan

DHPCGMA was synthesized following the procedure of Reis et al. (2006). 6.0ml distilled water and 4.0mL DMSO was used to prepare aqueous-DMSO solution. After complete homogenization, 1.0g of water soluble chitosan (WSC) was added to the DMSO/H_2O solution. 0.15mL TEMED and 1.0mL GMA was added to the WSC-DMSO/ H_2O solution. The resulting mixture was placed under continuous stirring at 40°C for 66 h and purification of the modified DHPCGMA was done using excess acetone. The precipitate was dissolved in water and re-precipitated with acetone and filtered. The precipitate was dried for 48 h.

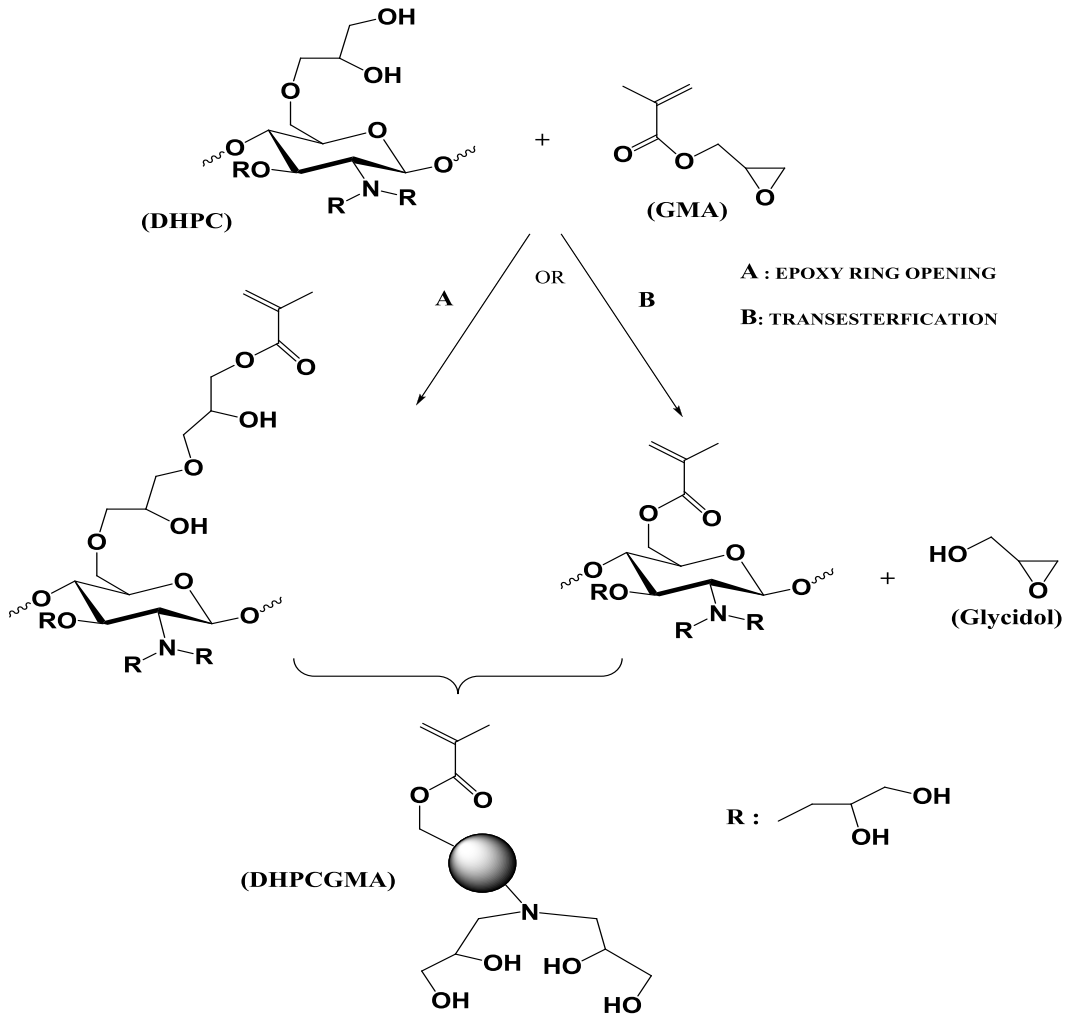

Scheme 3: schematic pathway for the synthesis of *N*, *O*-(2, 3 dihydroxypropyl) chitosan-GMA

2.2.2 Preparation of (DHPC-GMA-g-PAAm) superabsorbent hydrogel

0.5g DHPC-GMA was dissolved in 20.0mL water in a flask and left for 48 h to dissolve with continuous stirring. 0.02g of potassium persulfate and varying amounts of AAm monomer were added to four different portions of the dissolved solution in test tubes. The test tubes were placed in oil bath preset at 65°C and were allowed to stir for 60min. The gelation was observed after around 50min of heating. The hydrogels in each tube were washed in plenty of distilled water for 1day at room temperature, and then the hydrogels were dried at 60°C for 3days. Table 9 shows the

summarized amount of AAm, DHPC-GMA and KPS used for the synthesis of superabsorbent hydrogels at 65°C.

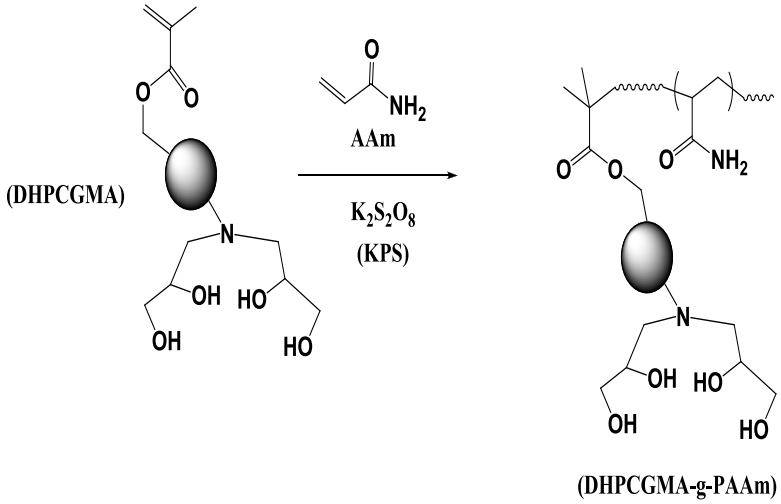

Scheme 4: Outline of the synthesis of *DHPC-GMA-g-PAAm* superabsorbent hydrogel

Table 3: Amount of AAm, DHPC-GMA and KPS used for the synthesis of hydrogels

Sample	DHPC-GMA (g)	AAm (g)	(g DHPC-GMA /gAAm)	KPS (g)
A	0.1	0.1	1	0.02
B	0.1	0.3	1/3	0.02
C	0.1	0.5	1/5	0.02
D	0.1	1	1/10	0.02

2.3 Instrumental Analysis

2.3.1 FT-IR spectroscopy

FT-IR spectra of chitosan, DHPC, GMA, DHPC-GMA and DHPC-GMA hydrogels were taken on a PerkinElmer FT-IR model 65 spectrometer. Powdered samples were prepared into pellets with KBr.

2.4 Investigation of swelling behavior

The water absorption of superabsorbent DHPC-GMA hydrogel was examined by water uptake capacity. Immersion of 1.1g of hydrogel in 40mL of distilled water was done at 25°C for 3days until the swelling equilibrium was achieved. The hydrogel weight increase allowed the calculation of the swelling percentage using the following equation:

$$\text{Swelling ratio (\%)} = \frac{Ws - Wd}{Wd} \times 100 \qquad (1)$$

Where Ws and W_d are the weights of the swollen gel and dry gel samples respectively. The effect of variable conditions such as acrylamide/WSC ratio, time, on hydrogel swelling behavior was also examined. When studying one factor, the other variable conditions were kept constant.

The kinetics of water absorption by DHPC-GMA-g-PAAm was investigated using the first order and pseudo- second order models according to the equations (2) and (3) respectively below:

$$\ln(S_e - S_t) = \ln S_e - k_1.t \qquad (2)$$

$$\frac{t}{S_t} = \frac{1}{k_2 S_e 2} + \frac{t}{S_e} \qquad (3)$$

Where t is time, S_e, S_t is the amounts of water absorbed onto DHPC-GMA-g-PAAm hydrogel at equilibrium and at time t respectively. Also, k_1 and k_2 are the absorption rate constants of pseudo-first-order and pseudo-second-order respectively.

2.5 Investigation of dye removal

2.5.1 Dye adsorption batch experiment

The dye adsorption experiment was performed using the standard batch technique on a shaker at 120rpm regular speed in 50mL flasks with a stopper. The Reactive Blue 2 (RB) and Erichrome Black T (EBT) used were of analytical grade. Their physicochemical characteristics are given in Table 4.

Table 4. The physicochemical characteristics of the dyes used.

Name	**Molecular structure**	M_W **(g/mol)**	λ_{max} **(nm)**
Eriochrome Black T	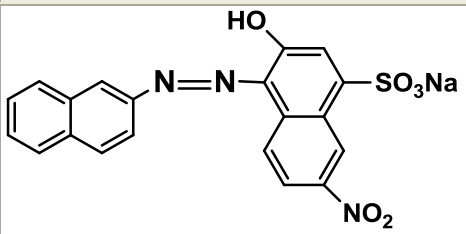	461.38	526
Reactive Blue 2	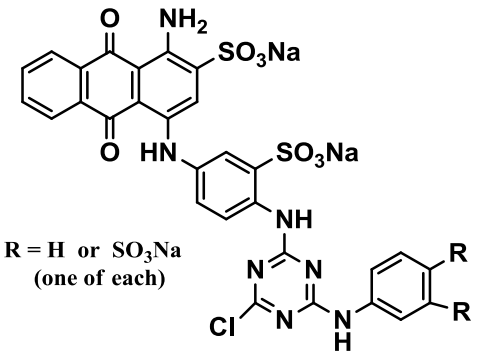	840.10	604

A known amount of each dye was dissolved in distilled water to prepare the stock solutions and the concentrations used finally were obtained by dilution of the stock solution. To study the adsorption capacity of DHPC-GMA hydrogel, RB and EBT removal from aqueous solution, batch experiments were performed with 25mL EBT and 25mL RB solutions of 100ppm both and 0.025g adsorbent in RB solutions and 0.025g adsorbent in EBT system. The mixture of the adsorbent and dye solutions was agitated for 74 h. The spectro-photometric analyses of the concentration of the dyes in the adsorption medium were done at the highest absorption wave length of 604 nm

and 526 nm for RB and EBT respectively using UVWin 5.0 spectrophotometer. Curves for calibration were plotted between absorbance and RB, EBT concentrations. The adsorption amount of RB and EBT, q_e was computed through this equation as follows:

$$q_e = (Co - Ce) \times \frac{V}{W} \quad (4)$$

Where the initial dye concentration (mgL^{-1}) is C_0, the equilibrium dye concentration (mgL^{-1}) is C_e, V (L) is volume of dye solution used and W (g) is the weight of the adsorbent used.

2.5.2 Adsorption kinetics

The rate of adsorption of dye onto the synthesized hydrogel and the efficiency of the adsorbent can be ascertained through kinetic studies. The kinetics of sorption can be followed using two kinetic models namely the pseudo-first-order and pseudo-second-order kinetics as expressed in the following equations:

$$\ln(q_e - q_t) = \ln q_e - k_1 t \quad (5)$$

$$\frac{dq_t}{dt} = k_2 (q_e - q_t)^2 \quad (6)$$

$$\frac{t}{q_t} = \frac{1}{k_2 q_e^2} + \frac{t}{q_e} \quad (7)$$

Where the rate constants for pseudo-first is k_1 and that of second-order adsorption is k_2, the amount of dye adsorbed (mgg^{-1}) at equilibrium is q_e while the amount of dye adsorbed at time t is given as q_t. From equations given above the slope and intercept of the plot of t/qt with time t in Eq. (7) gives the values of the k_2 and the intercept is equivalent to the q_e. RW is the characteristic kinetic curve of dye adsorption [52].

$$Rw = \frac{1}{1 + k t q_e t r} + \frac{t}{q_e} \quad (8)$$

The longest operation time is represented as t_r while the characteristic kinetic curve is referred to as approaching equilibrium when R_W is ranged within $0.1 < R_W < 1$.

2.5.3 Competitive Adsorption of dye mixtures

In the competitive adsorption experiments of dye mixtures, a mixture of 0.025g DHPC-GMA-g-PAAm hydrogel and 25mL mixture of dye solution (RB and EBT of equal proportions) was agitated for 74 h at constant speed of 120rpm. The spectro-photometric analyses of the concentration of the dyes in the adsorption medium were done at the highest absorption wave length of 604 nm and 526 nm for RB and EBT respectively using UVWin 5.0 The total absorbance and the adsorption kinetics of the mixture of the two dyes onto the superabsorbent hydrogel were studied according to the procedure in the literature [53]. According to Skoog, the total absorbance for a mixture of dyes is equal to the total absorbance of each dye if there is no chemical interaction between the two dyes and this can be obtained according to the equations below:

$$\mathbf{A}_{\lambda} = A_{\lambda RB} + A_{\lambda EBT} \quad (9)$$

$$\mathbf{A}_{\lambda 1} = \varepsilon_{\lambda 1 RB}\, \mathbf{c}_{\lambda 1 RB}\, \boldsymbol{l} + \varepsilon_{\lambda 1 EBT}\, \mathbf{c}_{\lambda 1 EBT}\, \boldsymbol{l} \quad (9a)$$

$$\mathbf{A}_{\lambda 2} = \varepsilon_{\lambda 2 RB}\, \mathbf{c}_{\lambda 2 RB}\, \boldsymbol{l} + \varepsilon_{\lambda 2 EBT}\, \mathbf{c}_{\lambda 2 EBT}\, \boldsymbol{l} \quad (9b)$$

In Eqs. 9 $\mathbf{A}_{\lambda}$, $\mathbf{A}_{\lambda 1}$, $\mathbf{A}_{\lambda 2}$ are the absorbance at wavelengths $\boldsymbol{\lambda}$, $\boldsymbol{\lambda}1$ and $\boldsymbol{\lambda}2$ respectively; $A_{\lambda RB}$ and $A_{\lambda EBT}$ are the absorbance of RB and EBT at wavelength $\boldsymbol{\lambda}_{RB}$ and $\boldsymbol{\lambda}_{EBT}$ respectively; $\boldsymbol{\varepsilon}_{\boldsymbol{\lambda 1}\,RB}$ and $\boldsymbol{\varepsilon}_{\boldsymbol{\lambda 2}RB}$ are the absorbance coefficient of pure RB at wavelength $\boldsymbol{\lambda}1$ and $\boldsymbol{\lambda}2$ respectively; $\boldsymbol{\varepsilon}_{\boldsymbol{\lambda 1}EBT}$ and $\boldsymbol{\varepsilon}_{\boldsymbol{\lambda 1}EBT}$ are the absorbance coefficient of pure EBT at wavelength $\boldsymbol{\lambda}1$ and $\boldsymbol{\lambda}2$ respectively; $\mathbf{c}_{\lambda RB}$ and $\mathbf{c}_{\lambda EBT}$ are the concentration of RB and EBT in the mixture solutions; $\boldsymbol{l}$ is the cell size (1 cm); $\boldsymbol{\lambda}1$ (604nm) is the

wavelength of maximum absorbance for RB; and λ2 (526nm) is the wavelength of maximum absorbance for EBT. The concentrations $c_{\lambda RB}$ and $c_{\lambda EBT}$ are solved from Eqs. (9a) and (9b) and then calculated to obtain the adsorption capacity for each dye in the mixture solutions.

Chapter 3

RESULTS AND DISCUSSION

3.1 Synthesis

The chemical modification of DHPC with GMA has been assumed to occur either through epoxy ring opening or transesterification reaction pathways [54]. The schematic representation of the possible reaction routes is shown in scheme 3. Research has shown that when DHPC is treated with protic solvent such as water, the DHPC will react with GMA through epoxy ring opening and the whole GMA molecules are anchored to the DHPC structure. With an aprotic solvent such as DMSO, the possible modification route of the DHPC with GMA is transesterification where glycidol is formed as by-product [55].

In this present work, calculated volume of water and DMSO was used during the modification stage and the main purpose of this work is to incorporate GMA vinyl groups onto the DHPC structure to form DHPC-GMA hydrogel and not to verify the reaction pathways. Potassium per sulfate (KPS) was used as an initiator to graft AAm onto DHPC-GMA. Active sites are generated via decomposition of the persulfate to produce sulfate radical which abstracts hydrogen from the OH group of DHPC-GMA. Then grafting reaction takes place from the active site created.

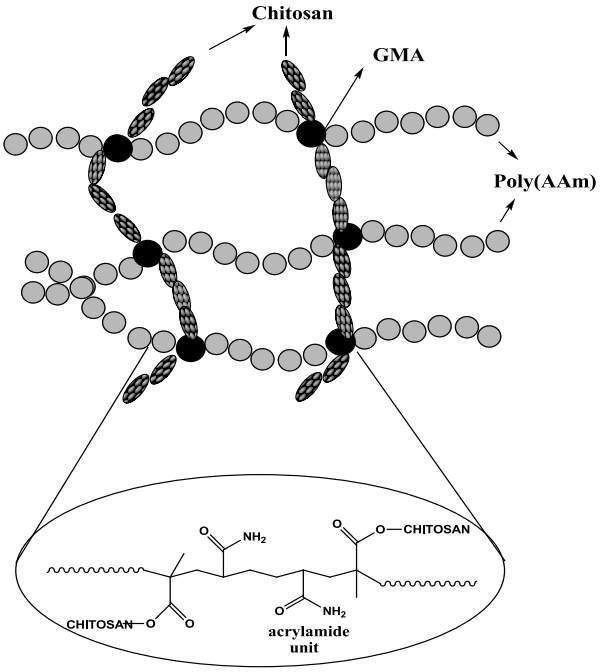

Figure 1. Schematic illustration of the SAH networks

DHPC-GMA grafted poly (acrylamide) with different grafting ratio and efficiency were prepared by using known amounts of DHPC-GMA (B, C and D), AAm and KPS at known temperature for 2 h. Calculated amounts of DHPC-GMA was dissolved in 15mL distilled water and the solution was divided into three portions containing 5mL solution each then varying amounts of monomer (AAm) were added to each solution under continuous stirring. 0.02g potassium persulfate was added to the mixture in a thermostatic oil bath for 1 h. The final reaction mixtures were poured into clean test tubes each in oil bath preset at 65^{o}C. For 2 h grafting reaction was allowed to occur and then reaction mixtures were precipitated using acetone to separate DHPC-GMA-g-PAAm from the homopolymers. The reagents details used for the experiments are shown in Table 5.

Table 5: Experimental details for the synthesis of DHPC-GMA grafted poly (acrylamide)

Experimental conditions for the synthesis of DHPC-GMA grafted poly (acrylamide)

Temperature: 65°C Time: 2h Potassium persulfate= 0.02g

DHPC-GMA-PAAm	DHPC-GMA (g)	AAm (g)	Grafted Copolymer (g)	G%	E%
B	0.1	0.3	0.2495	150	49.8
C	0.1	0.5	0.4038	304	60.8
D	0.1	1.0	1.0950	995	99.5

Note: 15 mL of distilled water was used for all the experiments.

The superabsorbent hydrogels prepared were dried at 60°C for 72 h to avoid hydration. The evidence of grafting was obtained by comparing FT-IR spectra analysis of DHPC-GMA and grafted copolymer as shown in section 3.2.1. The effect of monomer concentration was examined to show the swelling behavior of the prepared superabsorbent hydrogel and the grafting percentage and efficiency were determined using the following equations;

$$\text{Grafting (\%)} = \frac{W1-W0}{W0} \times 100 \quad (10)$$

$$\text{Efficiency (\%)} = \frac{W1-W0}{W2} \times 100 \quad (11)$$

The weights of the initial DHPC-GMA, grafted copolymer and the monomer used can be represented as W_0, W_1 and W_2 respectively.

3.1.1 Effect of AAm concentration on Grafting percentage and efficiency

The effect of AAm concentration on the grafting parameters was investigated by varying the amount of AAm during each grafting procedure.

The grafting parameters value increase with increase in the molarities of the AAm until 99.5% grafting efficiency and 995% grafting percent with 1.0g acrylamide and

0.1g DHPC-GMA. The increase in the AAm concentration provides a greater availability of AAm monomer to react with DHPC-GMA backbone leading to higher grafting efficiency and percentage.

This increase in grafting parameters with the increase in AAm concentration may be due to the formation of more monomer radicals which in turn generate more grafting sites on DHPC-GMA by the abstraction of the H atom or accumulation of the monomer molecules in the vicinity of DHPC-GMA, which increase the chance of the molecular collision and hence result in higher grafting.

3.2 Characterization

3.2.1 FT-IR analysis

The FT-IR spectra of chitosan, DHPC and DHPCGMA are depicted in figure 2. The IR spectrum of the chitosan showed strong peaks at 1030, 1082 and 1381cm^{-1} which could be assigned to the saccharide structure of the chitosan that is the O-H bending, C-O stretching and C-N stretching respectively.

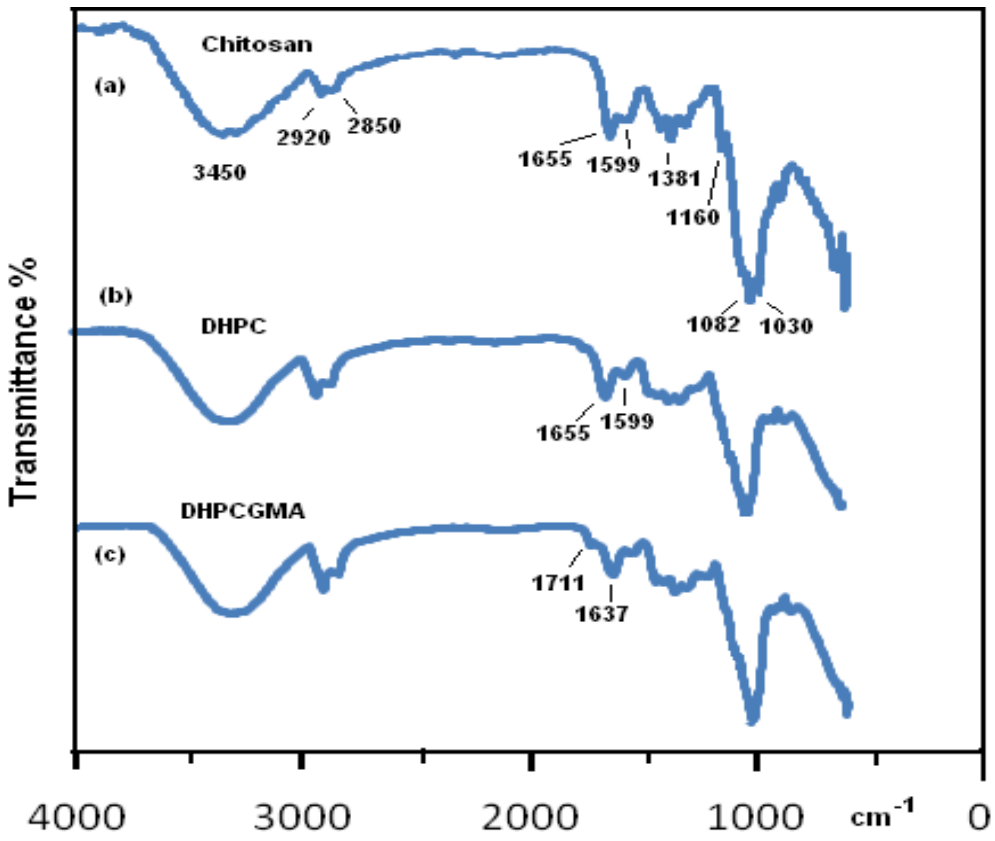

Figure 2. Transmittance FT-IR spectra of chitosan, DHPC and DHPCGMA

The peaks at 1655 and 1599 cm^{-1} could be attributed to the C=O stretching (amide I) and N–H (amide II) respectively. In the IR spectra of the DHPC, the absorption peaks at 1030 and 1160 cm^{-1} disappeared which are corresponding to C–O stretching of 3-OH and 6-OH of chitosan respectively. The disappearance of the peaks indicate that the hydroxypropyl substitution occurred at both 3-OH and 6-OH groups [56]. Also the characteristic peaks at 1599 cm^{-1} were weakened substantially, which indicates a decrease in –NH2 group content [57]. This structural elucidation revealed that both the OH groups at C-6 and C-3 and the NH_2 group could be alkylated under the experimental conditions. In the spectrum of DHPCGMA, new absorption peaks appeared at 1711 and 1637cm^{-1} which corresponds respectively to the carbonyl stretching C=O of the conjugated ester and C=C stretching frequency. The C=C

group was introduced into the DHPC chain after reaction with GMA and this is indicative of methacrylated modification of DHPC.

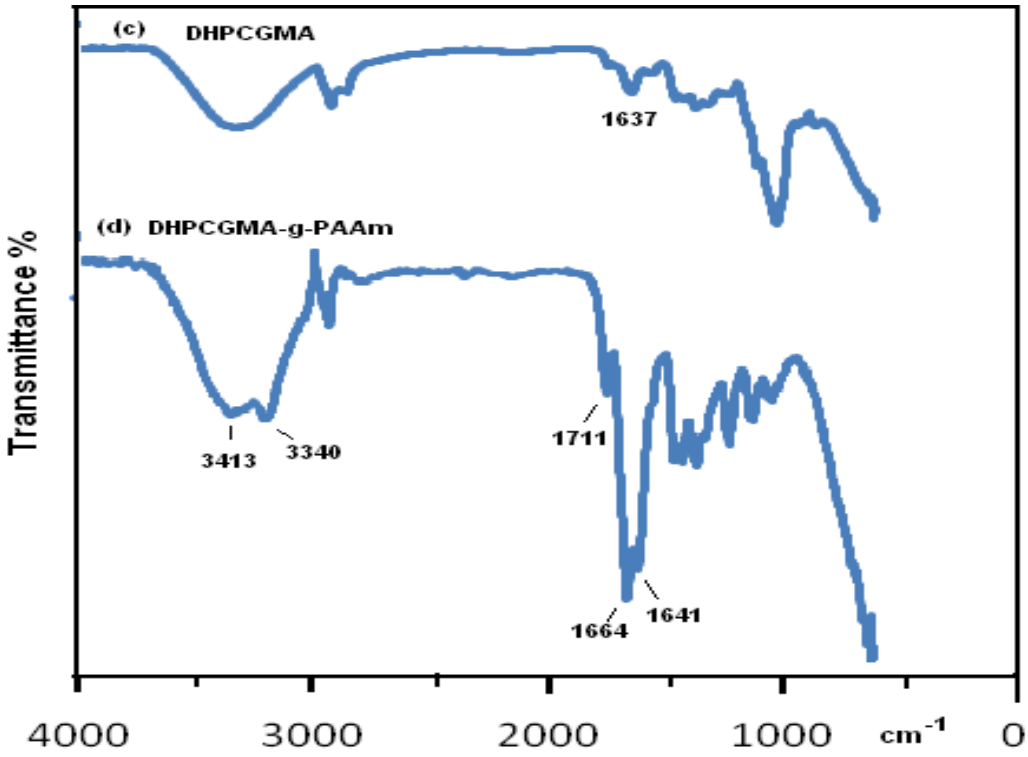

Figure 3. Transmittance FT-IR spectra of DHPCGMA and DHPCGMA-g-PAAm

The spectrum of the synthesized DHPCGMA-g-PAAm shows additional strong peaks at 1664 (amide I) and 1641cm^{-1} (amide II) respectively due to the grafted PAAm chains onto the DHPCGMA backbone while two peaks of O-H and N-H stretching in the grafted hydrogel are seen at 3413 and 3340cm^{-1} respectively and this is indicative of copolymerizing reaction of DHPCGMA with AAm.

3.3 Swelling behavior

The swelling behavior of superabsorbent hydrogels are greatly influenced by factors such as polymer composition, swelling media, immersion time, absorbent specific size area and various other reaction conditions. The effects of immersion time,

monomer ratio and pH were studied to investigate the swelling behavior of the synthesized superabsorbent hydrogel.

A B C

Figure 4. Photo of (A) dried hydrogel (B) Swollen hydrogel (C) Swollen D, C B hydrogels

3.3.1 Swelling of DHPC-GMA-g-PAAm Hydrogel in Water

The swelling capacity of hydrogels (B, C, D) during 50 h immersion in distilled water is shown in Fig.5 below. The swelling percentage was increased up to 10 h, then large difference in water uptake were not observed with further increase in time and it reached a state of equilibrium. The maximum swelling percentages of 1897.2%, 1507.1% and 1432.2% for D, C and B respectively were achieved after 50 h due to great hydrophilicity of polyacrylamide chains in the superabsorbent hydrogel backbone and the greater water holding capacity of DHPC-GMA-g-PAAm. This behaviour can be linked to weakening of hydrogen bonding and dissolving of grafted samples in the immersed water.

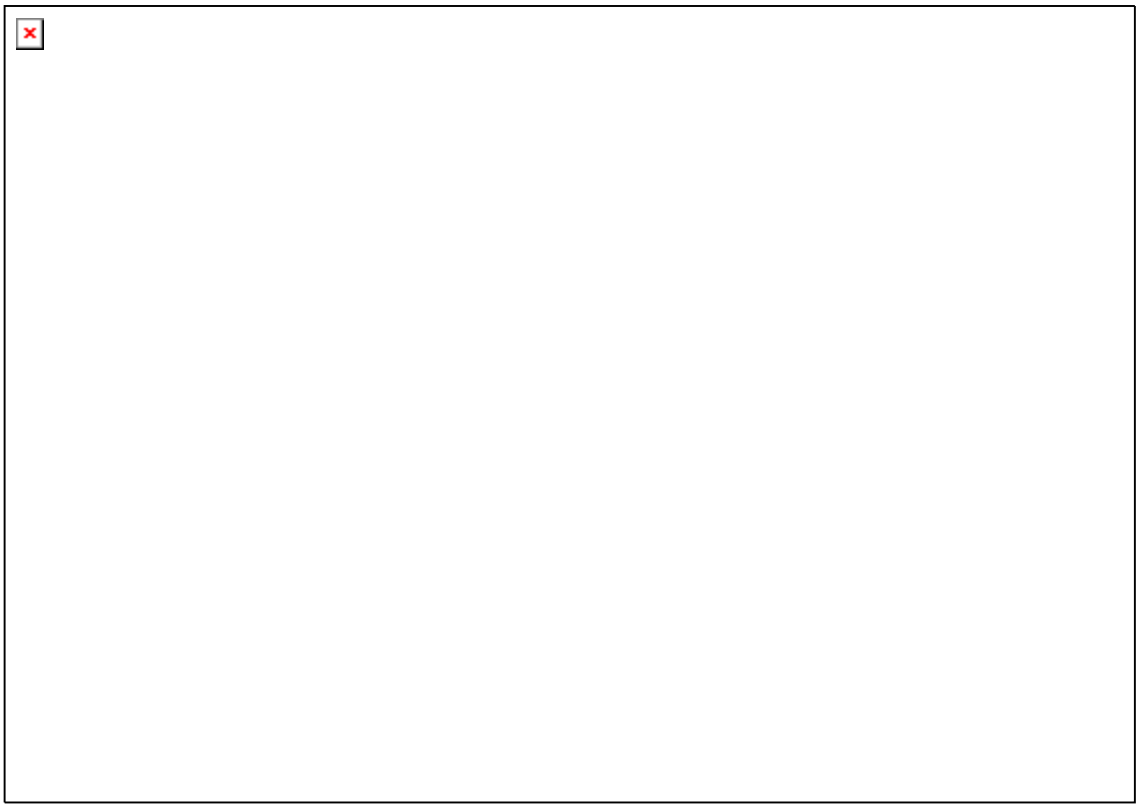

Figure 5. Swelling percentage for hydrogels B, C and D

3.3.2 Swelling kinetics of DHPC-GMA-g-PAAm Hydrogel

In order to investigate the swelling mechanism of DHPC-GMA-co-AAm hydrogel the swelling kinetics were investigated. The large number and series of different chemical units on the polymer chains of DHPC-GMA-g-PAAm networks implied various types of polymer–solvent interactions. The first order swelling kinetic was investigated using Eq. 12 and the data obtained can be found in Table 6 below, but the swelling process did not follow the first-order swelling kinetics.

$$\ln(S_e - S_t) = \ln S_e - k_1 t \qquad (12)$$

Therefore, to test the second order kinetics which controls the swelling process [17] the following equation was expressed as;

$$\frac{ds}{dt} = k_2 (s_e - s_t)^2 \qquad (13)$$

Where k_2 is the rate constant, S_t and S_e are water content at time t and equilibrium swelling ratio respectively. The integration of Eq. 13 when the initial conditions are applied, the equation becomes

$$\frac{t}{s_t} = \frac{1}{k_2 s_e 2} + \frac{t}{s_e} \qquad (14)$$

The swelling kinetic modelled as second order is shown in Fig.4. As it is seen from Fig.6 and by means of Eq.13, the swelling data shows straight line in the plot of $\frac{t}{s_t}$ against time with the slope and intercept of $\frac{1}{s_e}$ and $\frac{1}{k_2 s_e 2}$, respectively. Although, the theoretical s_e are 1897.2%, 1507.1% and 1432.2% for D, C and B respectively, and the observed values are 19.043 g/g (1904.3 %), 15.161g/g (1516.1%) and 14.531g/g (1453.1%) respectively for D, C and B. The correlation coefficients and the adsorption rate constants are tabulated below. As tabulated in Table 6, the R^2 shows higher values for pseudo-second-order model as compared to those of the pseudo-first-order, this is indicative of pseudo-second-order kinetics for water uptake capacity by DHPC-GMA-g-PAAm hydrogel and also the s_e values from the pseudo-second-order shows close proximity with those of the theoretical s_e validating the results.

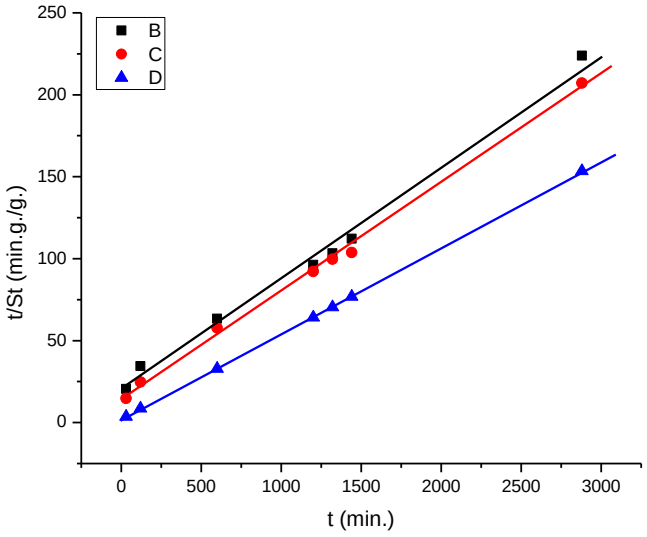

Figure 6. Swelling kinetic for hydrogel B, C and D in distilled water through pseudo-second-order

Table 6: Pseudo-first and second-order sorption kinetics of DHPC-GMA-g-PAAm hydrogel in water

Second-order sorption kinetic data				
DHPC-GMA-g-PAAm	s_e (g/g)	$k_2 \times 10^{-4}$ (min^{-1})	R^2	G%
B	14.531	2.521	0.99052	150
C	15.161	3.059	0.99677	304
D	19.043	0.168	0.99987	995
First-order sorption kinetic data				
DHPC-GMA-g-PAAm	s_e (g/g)	$k_1 \times 10^{-3}$(min^{-1})	R^2	G%
B	19.069	4.000	0.90231	150
C	17.196	3.300	0.70542	304
D	8.9131	4.300	0.99296	995

3.3.3 Effect of time on swelling capacity

The swelling behavior of DHPC-GMA-g-PAAm superabsorbent hydrogel was investigated at range of time. The change in water absorption capacity of the

hydrogels with time is shown in Fig.7 below. The Fig.7 below shows absorption of water by DHPC-GMA-g-PAAm during 3.0×10^{3}min.

The water uptake increased rapidly and after 6.0×10^{2}min it slightly reached equilibrium. As mentioned above, at 3.0×10^{3} min the highest swelling capacity of DHPC-GMA-g-PAAm was attained after immersion of the hydrogels in water. The swelling can be assigned to cross-linked polyacrylamide chains in the hydrogel having a large hydrophilic content, the degree of cross linking of DHPC-GMA/PAAm network and the higher capacity of PAAm present in the superabsorbent hydrogel, which has an increased number of water-binding sites [43].

Figure 7. Water uptake of DHPC-GMA-g-PAAm as a function of time

There is easy penetration of the water molecules within the hydrogel chain and this led to enhancement of the hydrogel features in solution. Initially according to Fig. 5, the percentage of swelling shows rapid increment. After which it blends to equilibrium level. The swelling equilibrium state of the DHPC-GMA-g-PAAm superabsorbent hydrogel immersed in distilled water was obtained when the solvent

inside the hydrogel network is in thermodynamic equilibrium with that outside and further increase in immersion time leads to maximum swelling percentage. Moreover, by comparing the theoretical equilibrium water absorption capacity with the experimental values in both models, the data obtained shows good agreement and conclusion can be reached that water absorption by DHPC-GMA-g-AAm hydrogel can be said to follow pseudo-second- order kinetic.

3.3.4 Effect of DHPC-GMA /AAm ratio on swelling percentage

The effect of DHPC-GMA /AAm ratio was investigated through changing the amount of the monomer to show the absorption characteristics in water from 0.1 to 1.0g whereas the amount of KPS and DHPC- GMA were kept constant. According to Fig 6, there is an increase in the swelling ratio (%) of DHPC-GMA-g-PAAm hydrogel as AAm amount increases to reach the highest value of swelling ratio (1877.2%) with sample D.

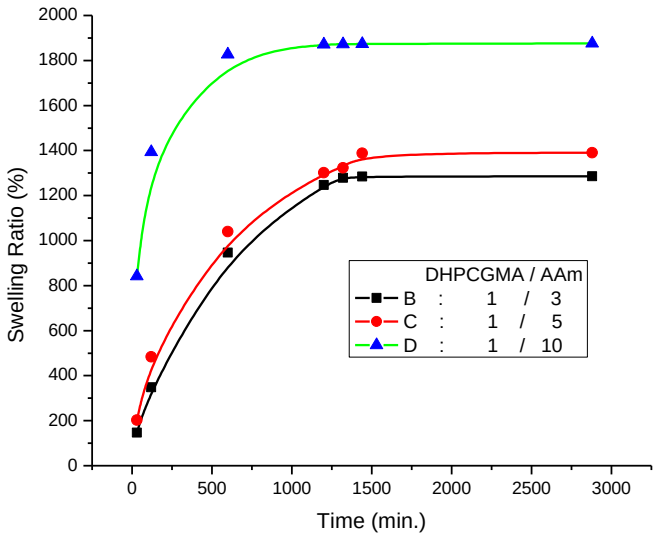

Figure 8. Effect of DHPC-GMA /AAm weight ratio on swelling kinetics of the superabsorbent hydrogels (reaction conditions: KPS= 0.02g, 65^0C, 120min).

The increase in water absorption with increase in acrylamide content may be attributed to higher concentration of the AAm molecules in the vicinity of the DHPC-GMA and this led to improved grafting on DHPC-GMA backbone and formation of good polymeric networks and greater percentage of swelling obtained.

3.4 Dye adsorption batch experiments

Dye experiment was conducted on a shaker at 120rpm for 72 h as described in section 2.5.1.The absorption capacity by the adsorbent after spectrophotometer reading was obtained by using the Eq. 15 below and dye solution concentration was obtained at wavelength corresponding to the highest absorbance of each dye.

$$qe = (Co - Ce) \times V/W \qquad (15)$$

The initial dye concentration (mgL^{-1}), equilibrium dye concentration (mgL^{-1}), volume of dye solution used and the weight of the adsorbent used are represented as C0, C_e, V (L), W (g) respectively.

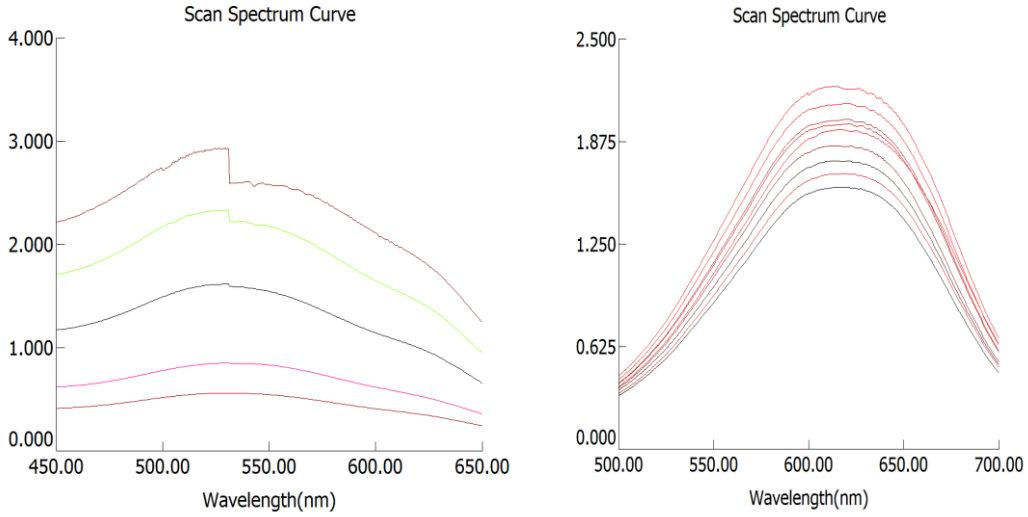

A B

Figure 9. UV-vis spectrum of scans (A) EBT (B) RB

3.4.1 Dye (RB and EBT) adsorption studies of DHPC-GMA-g-PAAm Hydrogel

The capacity of dye uptake by DHPC-GMA-g-PAAm hydrogel is calculated from Eq. 15 after determination of the dye concentration in solution after uptake with time. The present studies investigate the dye uptake capacity with time, variation of concentration with time for DHPC-GMA-g-PAAm and sorption kinetics for the dyes.

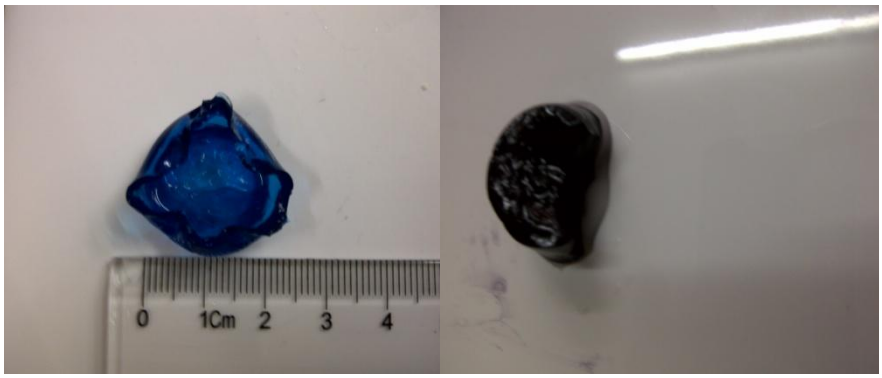

RB EBT

Figure 10. Photos of hydrogels loaded with Reactive Blue 2 (RB) and Erichrome Black T (EBT)

RB RB EBT

Figure 11. Photos of dye loaded hydrogels in distilled water

3.5 Adsorption kinetics

Investigation done on the relation between dye adsorption capacity and time shows that there is rapid binding of the dye to the hydrogel which was shown by the kinetic

data initially and then is followed by little increase till a state of equilibrium was obtained. The rapid stage initially can be attributed to higher number of vacant sites initially and improved concentration gradient between the dye in the gel and the dye in solution [37]. The adsorption parameters were followed by two kinetic models to understand the adsorption mechanism.

Table 7: Pseudo-first- and pseudo-second order sorption kinetics of Reactive Blue 2 (RB) and Erichrome Black T (EBT) on DHPC-GMA grafted poly (acrylamide): 100 ppm dye solution (25 mL) and 25 mg of adsorbent for all the experiments.

First-order sorption kinetic data RB					
DHPC-GMA-g-PAAm	q_e (mg/g)	$k_2 \times 10^{-3}$ (min^{-1})	R_w x10-^{4}	R^2	G%
B	48.611	1.47	0.648	0.985	150
C	35.905	0.90	1.939	0.949	304
D	19.305	2.63	2.297	0.813	995
First-order sorption kinetic data EBT					
DHPC-GMA-g-PAAm	q_e (mg/g)	$k_2 \times 10^{-4}$ (min^{-1})	R_w x10^{-3}	R^2	G%
B	7.153	9.427	4.648	0.980	150
C	10.807	6.809	2.824	0.787	304
D	26.691	18.600	0.169	0.991	995
Second-order sorption kinetic data RB					
DHPC-GMA-g-PAAm	q_e (mg/g)	$k_2 \times 10^{-5}$ (min^{-1})	R_w	R^2	G%
B	58.14	2.7026	0.125	0.995	150
C	48.96	3.6440	0.112	0.994	304
D	32.73	17.134	0.039	0.999	995
Second-order sorption kinetic data EBT					
DHPC-GMA-g-PAAm	q_e (mg/g)	$k_2 \times 10^{-4}$ (min^{-1})	R_w	R^2	G%
B	12.790	3.634	0.046	0.995	150
C	16.318	1.478	0.085	0.984	304
D	38.020	1.431	0.039	0.999	995

3.5.1 RB2 sorption kinetics

The kinetics of adsorption for Reactive Blue 2 (RB) onto DHPC-GMA-g-PAAm hydrogel was investigated as the data obtained from the studies will be useful to depict the adsorption efficiency and the data can be represented using two kinetic models, namely pseudo-first-order and pseudo-second-order as expressed in the equations below respectively.

$$\ln(q_e - q_t) = \ln q_e - k_1 t \qquad (16)$$

$$\frac{t}{q_t} = \frac{1}{k_2 q_e^2} + \frac{t}{q_e} \qquad (17)$$

Where t is time, the amounts of RB adsorbed onto DHPC-GMA-g-PAAm hydrogel at time t, at equilibrium and maximum adsorption capacity can be represented as q_t, q_e and q_e^2 respectively. Also, the adsorption rate constant of pseudo-first-order is k_1 and pseudo-second-order is k_2.

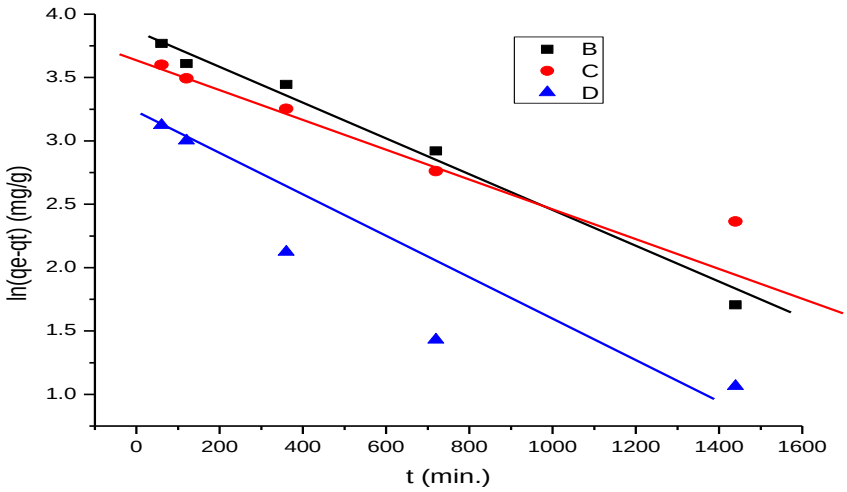

Figure 12. RB2 dye adsorption on hydrogels through pseudo-first order kinetic model

As shown in Figure 12, ln (q_e-q_t) against time (t) plot is a linear graph with slope and intercept giving k_1 and qe_1 respectively. The computed pseudo-first-order kinetic data are tabulated in Table 7 above.

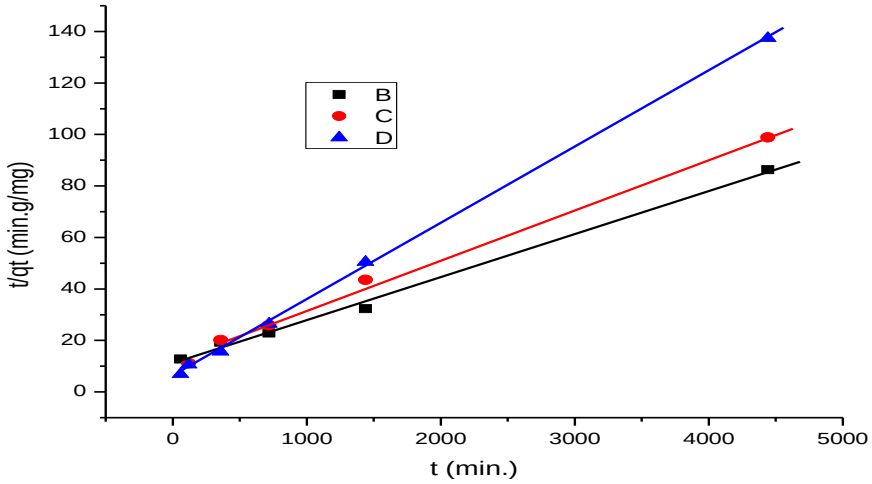

Figure 13. RB2 dye adsorption on hydrogels through pseudo-second- order kinetic model

Figure 13 is a straight line plot of $\frac{t}{q_t}$ against time t and this can lead to finding the adsorption constant k_2 and the highest amount of dye adsorbed qe_2 from the slope and intercept accordingly. Following the dye adsorption batch process for RB, the maximum RB adsorption onto DHPC-GMA-g-PAAm hydrogel after 74 h contact time are 50.06mg/g, 43.71mg/g and 31.46mg/g for B, C and D respectively. According to the obtained data as indicated in table 7, the values of R^2 were found to be higher in the pseudo-second-order when it's being compared to the pseudo-first-order. From the obtained data the first order kinetic data do not fit with the theoretical data and this shows the data obtained is model after pseudo-second-order kinetic for RB adsorption onto DHPC-GMA-g-PAAm hydrogel and also the q_e values obtained after computation through the pseudo-second-order equation indicate

close agreement with those of the experimental q_e as shown in Table 7 thereby validating the results as stated above. The first-order kinetic model has shown that equilibrium has been established between the RB dye solution and the DHPC-GMA-g-PAAm hydrogel, whereas pseudo-second-order indicates that the limiting step is chemical adsorption and the coefficient of correlation for the pseudo-second order almost equate to one in most cases and this means the adsorbent have high adsorption capacity with short equilibrium time which shows high degree of binding of the gel with the used dye, while Rw values obtained are also ranged within 0-1, meaning favourable adsorption process has occurred.

3.5.1.1 Effect of contact time

Experimental data of the adsorption of RB2 on DHPC-GMA-g-PAAm against time indicates decrease in dye concentration in solution as time of contact increases even though the amount of RB dye adsorbed on DHPC-GMA-g-PAAm increased with decrease in RB concentration in solution as shown in figure 14 below.

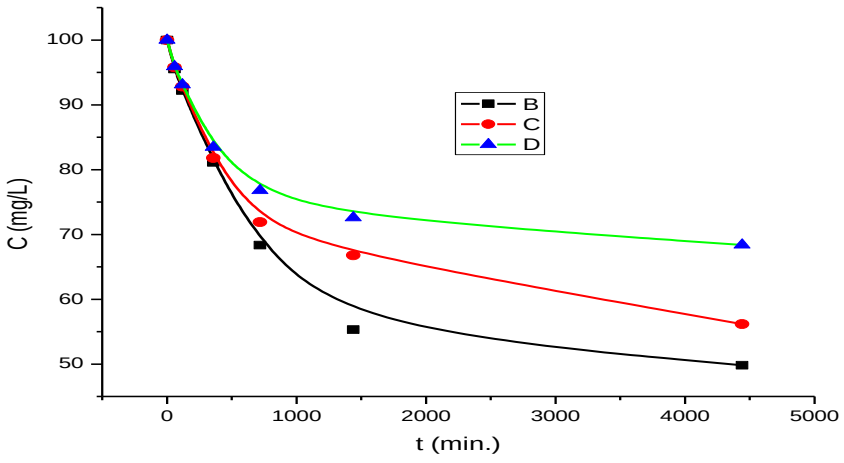

Figure 14. RB2 concentration in solution with time for DHPC-g-PAAm B, C, D of dye concentration

The equilibrium time for the maximum adsorption can be obtained if the adsorption uptake versus contact time was investigated as shown in figure 15. As indicated

below, there is a rapid increment in the adsorption capacity during the first range of time (0-1440min), but after the contact time reached 1440min with prompt increase in adsorption, the adsorption capacity almost remained same.

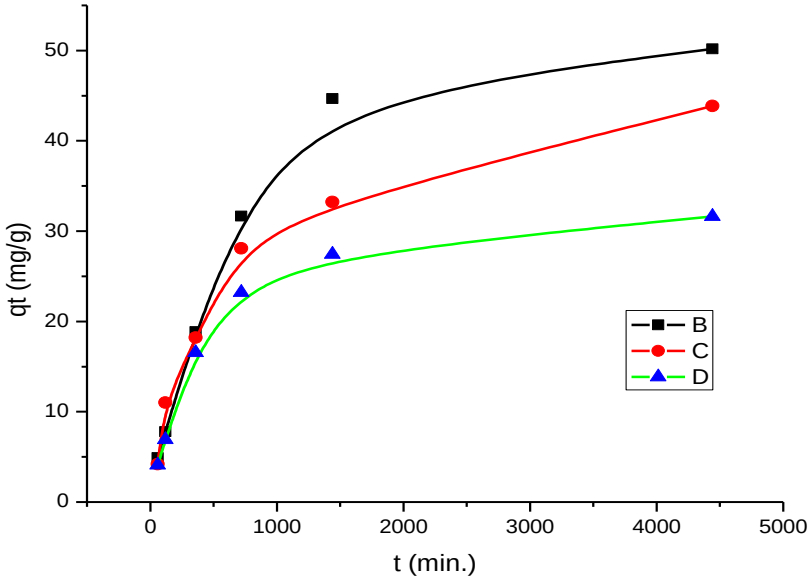

Figure 15. Contact time effect of RB on DHPC-GMA-g-PAAm B, C, and D adsorption

This shows that RB adsorption reached equilibrium time at 1440min as investigated. Finally, Fig. 15 is a continuous curve and this simply shows that the dye was saturated on the adsorbent, and this is an indication that the coverage of RB on the DHPC-GMA-g-PAAm is monolayer.

3.5.2 EBT sorption kinetics

The efficiency of adsorption of Erichrome Black T (EBT) onto DHPC-GMA-g-PAAm hydrogel was also investigated through the study of its kinetics and the two kinetic models were also applied to validate the results between the theoretical and experimental data.

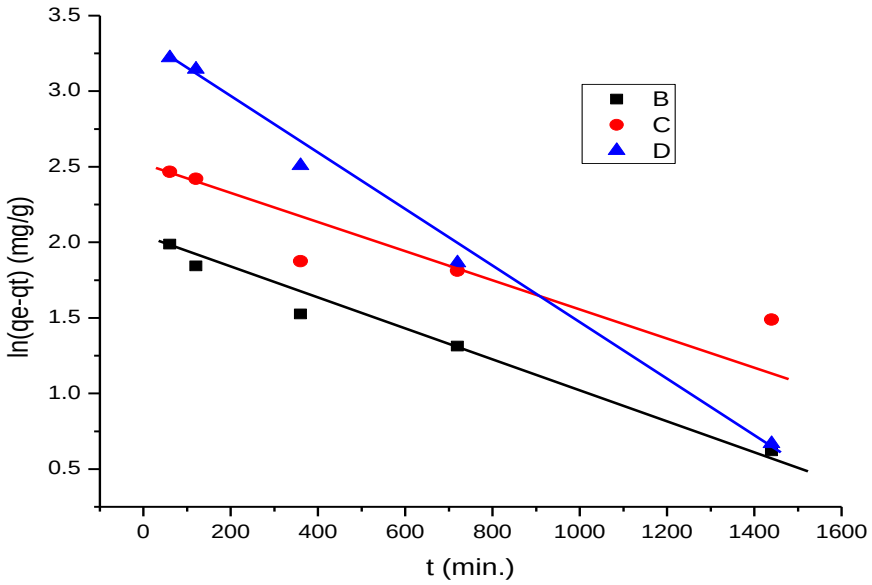

Figure 16. EBT dye adsorption on hydrogels through pseudo-first order kinetic model

As shown in Figure 16, ln (q_e-q_t) versus time (t) plot is linear with slope and intercept equal to k_1 and qe_1 respectively. The calculated pseudo-first-order kinetic data for EBT are tabulated in Table 14 above. The experimental data obtained for the EBT dye adsorption onto DHPC-GMA-g-PAAm are 12.34mg/g, 15.28mg/g and 36.44mg/g for hydrogels B, C and D respectively but the data does not fit well with the pseudo-first-order kinetic but only shows that equilibrium has being established between the EBT dye solution and the DHPC-GMA-g-PAAm hydrogel.

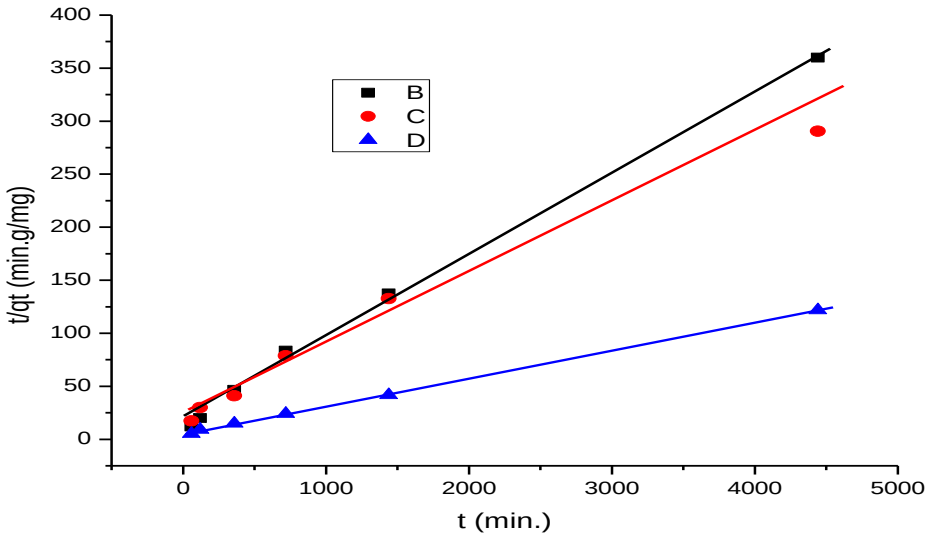

Figure 17. EBT dye adsorption on hydrogels through pseudo-second-order kinetic model

When the experimental data obtained after 74 h EBT dye solution contact time with the hydrogel is being compared with the calculated data, the R^2 indicates higher values through the pseudo-second-order model than those of the pseudo-first-order. Also after computation of the $\mathbf{q_e}$ values of EBT adsorbed on DHPC-GMA-g-PAAM hydrogel through the pseudo-second-order equation, its indicate close agreement with those of the experimental $\mathbf{q_e}$ as shown in Table 7 thereby validating the results as stated above.

This simply means that the pseudo-second-order kinetic model indicates that chemical adsorption occur at the rate limiting step. The correlation coefficients also tend towards unity for the pseudo-second-order kinetic model in most of the data obtained and this means the hydrogel shows high adsorption capacity at short equilibrium time and is an indication of high binding ability of the adsorbent with the

dye used. The R_w values are ranged within 0-1 which indicates favourable adsorption process.

3.5.2.1 Effect of contact time

Experimental data of the adsorption of EBT on DHPC-GMA-g-PAAm against time indicates decrease in dye concentration in solution as time of contact increases even though the amount of EBT dye adsorbed on DHPC-GMA-g-PAAm increased with decrease in EBT concentration in solution as shown in figure 18 below.

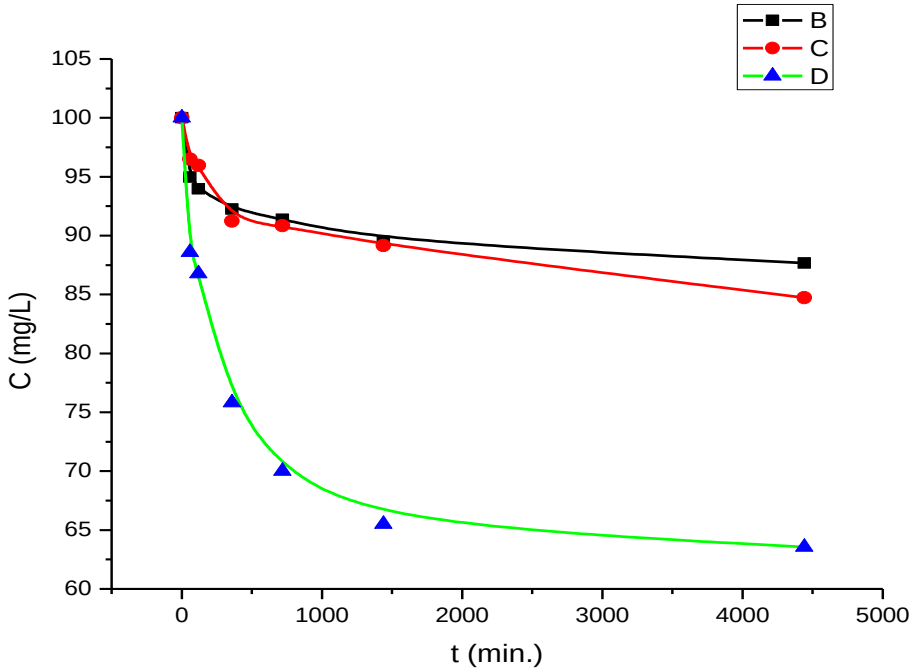

Figure 18. EBT concentration in solution with time for DHPC-g-PAAm B, C, D of dye concentration

The equilibrium time for the maximum adsorption can be obtained if the adsorption uptake versus contact time was investigated as shown in figure 19. As indicated below, there is a rapid increment in the adsorption capacity during the first range of time (0-360min), but after the contact time reached 360min with prompt increase in adsorption, the adsorption capacity almost remained same.

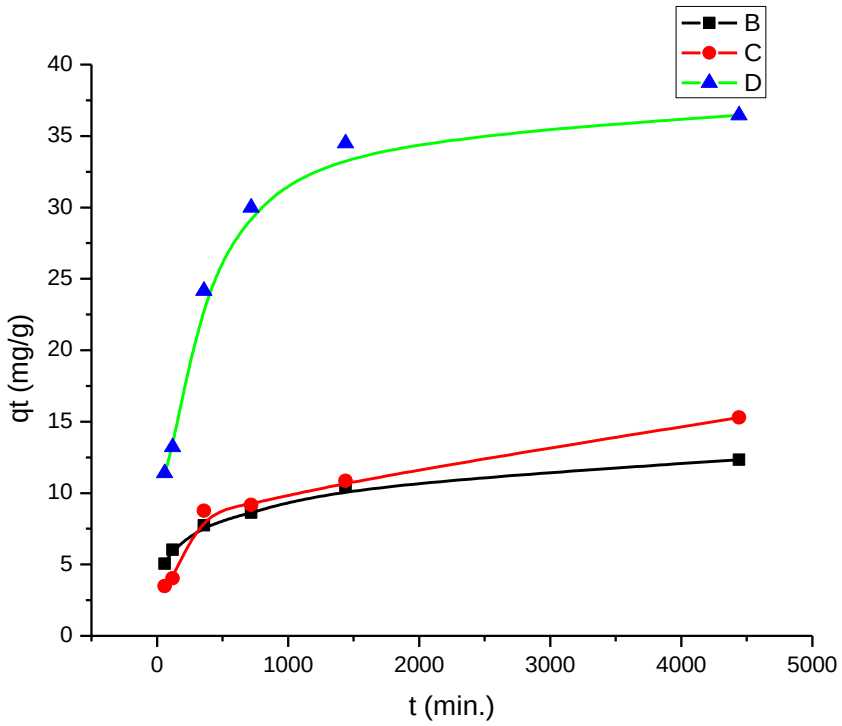

Figure 19. Contact time effect of EBT on DHPC-GMA-g-PAAm B, C, D adsorption

The EBT adsorption reached equilibrium time at 360min as investigated. Finally, Fig. 19 is a continuous curve and this means the dye was saturated on the adsorbent, and this suggests that EBT coverage on the DHPC-GMA-g-PAAm is monolayer.

3.5.3 Competitive Adsorption of dye mixtures (RB2 and EBT) by DHPC-GMA-g-AAm

To study the adsorption behavior of dye mixtures (RB2 and EBT) onto DHPC-GMA-g-PAAm, the adsorption kinetics of mixtures of the reactive and azo dyes onto the superabsorbent hydrogel was studied according to the procedure described by Skoog [53]. According to Skoog, the total absorbance for a mixture of dyes is equal to the total absorbance of each dye if there is no chemical interaction between the two dyes and the total absorbance and concentrations of RB2 and EBT can be obtained according to the equations given in section 2.5.3.

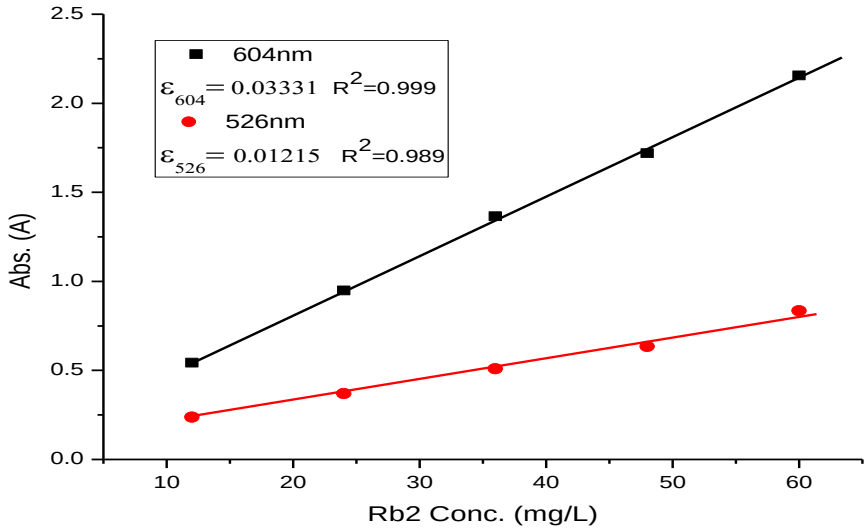

Figure 20. Absorbance of RB2 concentrations at different wavelengths

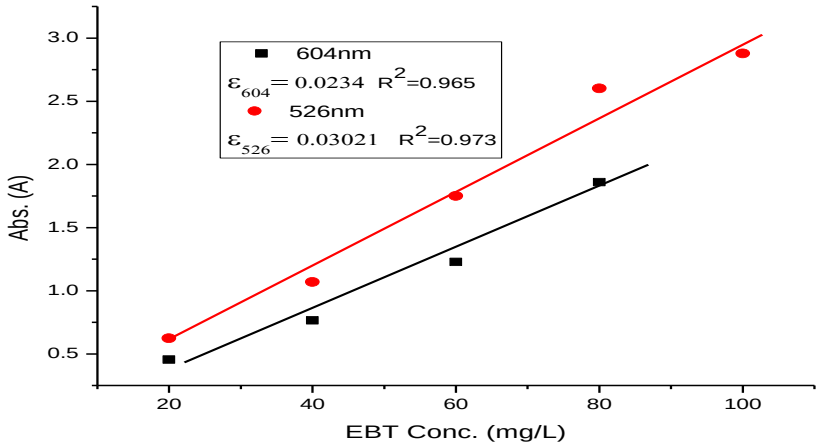

Figure 21. Absorbance of EBT concentrations at different wavelengths

3.5.3.1 Sorption kinetic for mixture of dyes (RB2 and EBT)

Sorption kinetics for mixture of dyes were investigated which was similar to the adsorption kinetics of a single dye discussed above. The kinetic of mixture of dyes can be described by the linear pseudo-first-order and pseudo-second-order kinetic models as tabulated below:

Table 8: Pseudo-first and second-order sorption kinetics of mixture of RB2 and EBT onto DHPC-GMA-g-PAAm

Second-order sorption kinetic data				
Dye	q_e (mg/g)	$k_2 \times 10^{-3}$ (min^{-1})	R^2	q_{eexp}(mg/g)
RB2	13.048	4.720	0.998	12.951
EBT	23.596	0.308	0.999	22.475
First-order sorption kinetic data				
Dye	q_e (mg/g)	$k_1 \times 10^{-3}$(min^{-1})	R^2	q_{eexp} (mg/g)
RB2	1.509	1.14	0.973	12.951
EBT	9.626	1.69	0.995	22.475

The adsorption capacity of each dye in the mixture was computed using Skoog procedure for mixture of dyes and the maximum dye uptake onto DHPC-GMA-PAAm was 22.475mg/g and 12.951mg/g for EBT and RB2 respectively. Figure 22 below shows that the initial adsorption rate for RB2 onto the DHPC-GMA-PAAm hydrogel was faster than that of the EBT but the amount adsorbed was much lower compared with EBT with slower adsorption rate but higher amount adsorbed onto the hydrogel.

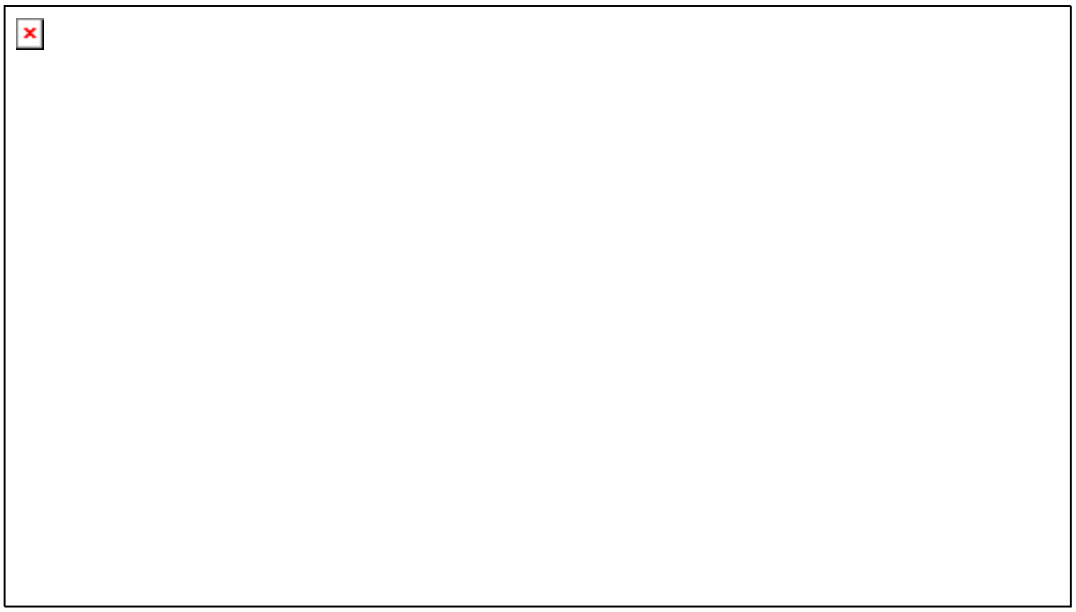

Figure 22. Mixture of RB2 and EBT dyes adsorption on hydrogel through pseudo-second-order kinetic model

This might be caused by the greater RB2 affinity with the hydrogel backbone. The RB2 has chlorotriazine group and this is responsible for the nucleophilic reactions with the functional units on the DHPC-GMA-g-PAAm chain, which provides fast binding sites for RB2 in the aqueous solution [47].

Table 8 above shows computed values of pseudo-first and pseudo-second-order kinetics and the experimental data when compared with the calculated data indicates that the obtained data cannot be fitted through pseudo-first-order model but through the pseudo-second order model. Also to validate the result, the k_2 rate constant for RB2 shows it was adsorbed faster than the EBT and the value of the correlation coefficients R^2 obtained tends towards unity which indicates favourable adsorption.

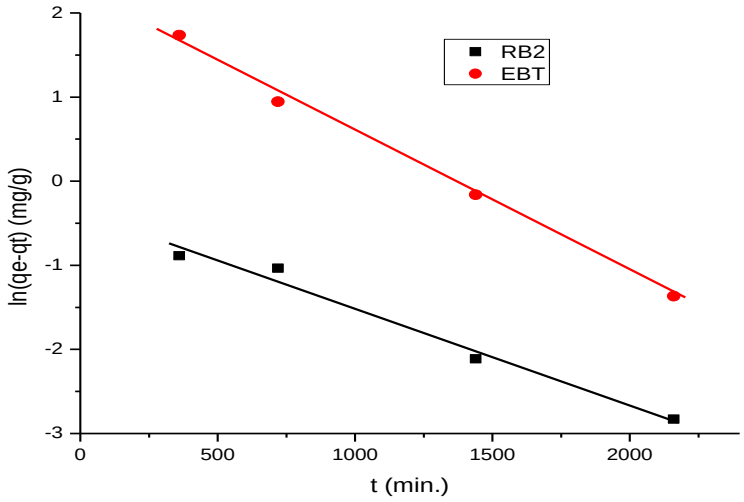

Figure 23. Mixture of RB2 and EBT dyes adsorption on hydrogel through pseudo-first-order kinetic model

3.5.3.2 Effect of contact time

In order to study the effect of contact time with the dye uptake capacity, the dye concentration behavior in solution was also investigated.

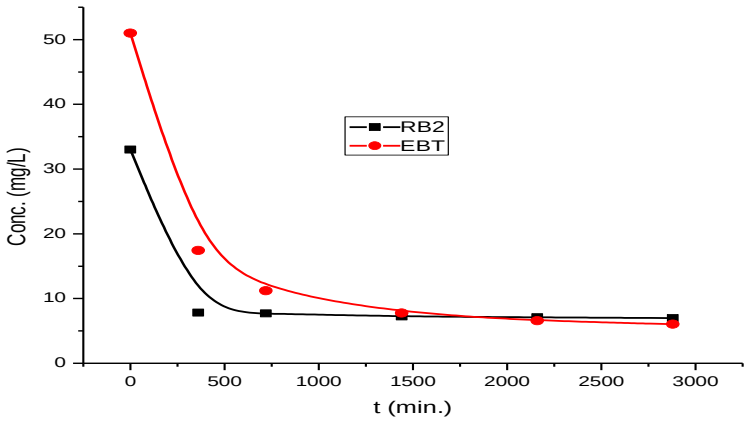

Figure 24. RB2 and EBT concentrations in solution with time for adsorption onto DHPC-GMA-g-PAAm, D

The adsorption rate of RB2 onto DHPC-GMA-g-PAAm is much faster than that of EBT as seen in Fig 24. The dyes concentration in solution decreases with time but the actual amount of the mixture of dyes adsorbed per unit mass of DHPC-GMA-g-PAAm increased with decreasing dyes concentration in solution.

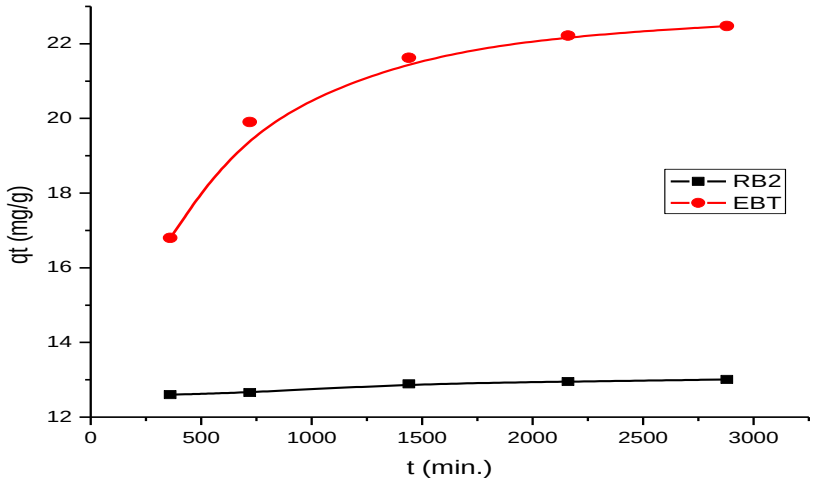

Figure 25. Effect of contact time of dye mixtures on DHPC-GMA-g-PAAm adsorption

The dye mixture of RB2 and EBT reaches the adsorption equilibrium at about 1480min with high amount of EBT adsorbed compared to the amount of RB2 adsorbed and this indicates that 1480min is the equilibrium time. Finally, Fig. 25 is a continuous curve which is a sign of saturation and monolayer coverage of RB2 and EBT on the DHPC-GMA-g-PAAm. To investigate which dye is more favourable in the competitive adsorption, the maximum single dye adsorbed was transferred into the ratio (single/mixture) of the adsorption capacity. The ratio of EBT reaches 63.4% at 48hr contact time that is larger than that of RB2 which is 36.5% within same contact time.

This shows that the adsorption kinetics of the two dyes influence each other and the competitive adsorption favours the dye EBT in the mixture solution onto DHPC-GMA-g-PAAM. Finally the molecular size of RB2 also affects the competitive amount of RB2 adsorbed in the solution.

Chapter 4

CONCLUSIONS

1) In this present study, successful synthesis of a superabsorbent hydrogel (DHPC-GMA-g-PAAm) was achieved through a two-step reaction process: water soluble chitosan (DHPC) was reacted first with glycidyl methacrylate (GMA) to produce DHPC-GMA, and then AAm and KPS were added to promote the polymerization with DHPC-GMA to produce the final superabsorbent hydrogel DHPC-GMA-g-PAAm.
2) FT-IR spectroscopies elucidate the structural changes in the materials and the results confirmed the successful incorporation of vinyl groups from GMA into the DHPC structure and strong interactions between DHPC-GMA and PAAm was observed.
3) The effect of DHPC-GMA/AAm weight ratio was examined on the swelling behavior of the synthesized superabsorbent hydrogel and the highest water swelling percentage (about 1900%) was obtained within the experimental reaction conditions: DHPC-GMA/AAm weight ratio = 0.1, KPS = 0.02g and reaction temperature 65^{o}C. The swelling mechanism indicates pseudo-second-order kinetic model with high water absorption uptake by the hydrogel.
4) The changes in the superabsorbent hydrogel morphology with GMA, *N*-*O*-HP and DHPC-GMA/AAm weight ratio indicates close agreement with the hydrogels B, C and D swelling behavior and the results suggest that these hydrogels can be useful in biomedical, Agricultural fields due to their greater

swelling ability in water and they were used as dye removal for Reactive Blue 2 (RB2) and Erichrome Black T (EBT) in this study.

5) In this study, three different grafted copolymer materials labeled B, C and D with varying grafting percentages were compared as sorbents for removal of Reactive blue 2 and Erichrome black T and the experimental observations are summarized below:

    - DHPC-GMA-g-PAAm with highest grafting percentage and efficiency (D- G%= 995 and E%= 99.5%) present highest sorption capacities for Erichrome black T (38.02mg/g) while sample B with lowest grafting percentage and efficiency (B- G%= 150 and E%= 49.8) present lowest sorption capacities for EBT (12.79mg/g).
    - DHPC-GMA-g-PAAm with lowest grafting percentage and efficiency (B-G%= 150 and E%= 49.8) present highest sorption capacities for RB2 (58.14mg/g) while sample D with highest grafting percentage and efficiency (D-G%= 995 and E%= 99.5%) present lowest sorption capacities for RB2 (32.73mg/g).
    - In the dyes mixture, the adsorption kinetics of the two dyes influence each other, competitive adsorption favors the dye EBT and the dynamic behavior for mixture of dyes adsorption onto DHPC-GMA-g-PAAM preferably obeyed pseudo-second-order-kinetics similarly to that of single dye sorption kinetics. The sorption rate was very fast for RB2 with lower adsorption capacity compared to EBT sorption process with higher adsorption.
    - The greater sorption sites due to higher grafting of sample D coupled with the charge interaction between the $-NH_3^+$ of chitosan and EBT anions can

be responsible for the high adsorption capacity of EBT onto the hydrogel, while the less columbic repulsion between the three sulphonic anions of RB2 and less amide groups of PAAm might cause the high sorption capacity of RB2 in sample B.

Table 9: Experimental and the kinetic data obtained during the research

Swelling behavior in water

Sample	*X*	*G%*	*E%*	S_{eexp} *mg/g.*	$S_{ecal.}$ *mg/g*	$K_2 \times 10^{-4}$ *(min^{-1})*	R^2
B	1/1	150	49.8	14.322	14.531	2.521	0.99052
C	1/3	304	60.8	15.071	15.161	3.059	0.99677
D	1/10	995	99.5	18.972	19.043	0.168	0.99987

Erichrome Black T

Sample	*X*	*G%*	*E%*	q_{eexp} *mg/g.*	$q_{ecal.}$ *mg/g*	$K_2 \times 10^{-4}$ *(min^{-1})*	R_w	R^2
B	1/1	150	49.8	12.34	12.790	3.634	0.046	0.995
C	1/3	304	60.8	15.28	16.318	1.478	0.085	0.984
D	1/10	995	99.5	36.44	38.020	1.431	0.039	0.999

Reactive Blue 2

Sample	*X*	*G%*	*E%*	$q_{eexp.}$ *mg/g*	$q_{ecal.}$ *mg/g*	$K_2 \times 10^{-5}$ (min^{-1})	R_w	R^2
B	1/1	150	49.8	50.06	58.14	2.7026	0.125	0.995
C	1/3	304	60.8	43.71	48.96	3.6440	0.112	0.994
D	1/10	995	99.5	31.46	32.73	17.134	0.039	0.999

Mixture of Reactive Blue 2 and Erichrome Black T

Sample	*Dye*	*G%*	*E%*	$q_{eexp.}$ *mg/g*	$q_{ecal.}$ *mg/g*	$K_2 \times 10^{-3}$ (min^{-1})	*X*	R^2
D	RB2	995	99.5	12.951	13.048	4.720	1/10	0.998
D	EBT	995	99.5	22.475	23.596	0.308	1/10	0.999

Where X = DHPCGMA/AAm, G% =grafting percentage, E%=efficiency, k= rate constant for second order kinetic, R^2 =correlation coefficient, R_w = characteristic of kinetic curve

REFERENCES

1. Buchholz F. L., Peppas N. A. (1994). Superabsorbent Polymer: Science and Technology, ACS Symposium Series 573, *Amer. Chem. Soci.* Washington, DC

2. Bajpai A. K., Giri, A. (2003). Water sorption behaviour of highly swelling (carboxy methylcellulose-g-polyacrylamide) hydrogels and release of potassium nitrate as agrochemical. *Carbohydrate Polymers*, 53(3), 271–279.

3. Crompton K.E, Prankerd R.J., Paganin D.M, Scott T.F., Horne M.K., Finkelstein D.I., Gross K.A., Forsythe J.S. (2005) Morphology and gelation of thermosensitive chitosan hydrogels. *Biophys Chem*.117:4.

4. Paulino A.T., Guilherme M.R., Reis A.V, Campese G.M, Muniz E.C, Nozaki J. (2006) Removal of methylene blue dye from an aqueous media using superabsorbent hydrogel supported on modified polysaccharide. *J Colloid Interface Sci.* 301:5.

5. Alessandro S., Christian D., Marta M., (2009) Biodegradable Cellulose-based Hydrogels: Design and Applications. *Materials.* 2:353-373

6. Buchholz F.L., Graham A.T., (1998) Modern Superabsorbent Polymer Technology, Wiley-VCH, New York, Ch 1-7.

7. Danya U, Mehta S.K., Choudhari M.S., Jain R, (1999) Synthesis of acrylic super absorbents, *J Macromol Sci-Rev Macromol Chem Phys,* Ch 39, 507-525,

8. Buchholz FL, Peppas NA, Superabsorbent Polymers Science and Technology, ACS Symposium Series, 573, American Chemical society, Washington, DC, Ch 2, 7, 8, 9, 1994

9. Flory, P.J., (1953) Principles of Polymer Chemistry; Cornell University Press: Ithaca, NY, 4: 342

10. Sannino A.S., Pappadà M., Madaghiele A., Maffezzoli L., Ambrosio L., Nicolais, (2005) Polymer 46 11206–11212

11. Qui Y., Oark K., (2001) Environment-sensitive hydrogels for *drug delivery. Adv Drug Delivery Rev*; 53:321.

12. Brannon P.L., Harland R.S., (1990) Absorbent Polymer Technology, *Elsevier*, Amsterdam, Ch 1-4.

13. Po R., (1994) Water-absorbent polymers: A patent survey, *J Macromol. Sci-Rev Macromol Chem Phys*, C34, 607-662,

14. Jayakumar, R.P.M., Reis R.L., Mano J.F. (2005). Graft Copolymerized Chitosan-Present Status and Applications. *Carbohydrate Polymers*, 62, 142-158.

15. Andrade J.D., (1976) Hydrogels for medical and related applications, *ACS Symp*. Series, 31, American Chemical Society, Washington DC, 1,

16. Zohuriaan-Mehr M.J, (2006) super absorbents. *Iran polym. Soci.* 2-4

17. Pokhrel D., Viraraghavan T., (2004) Treatment of pulp and paper mill wastewater-a review. *Sci Total Environ.* 333:37–58

18. Fereidoon S., Janak K.V.A., Jeon Y.J., (1999) Food applications of chitin and chitosans, *Trends in Food Science & Technology*, 10, No. 2, 37

19. Synowiecki J., Al-Khateeb N.A., (2003), Production, properties, and some new applications of chitin and its derivatives. *Crit Rev Food Sci Nutrition.* 43:145–171.

20. Ostanina E.S., Varlamov V.P., Iakovlev G. I., (2008) Inhibition of lipase activity by low-molecular-weight chitosan. *Prikladnaia biokhimiia i mikrobiologiia*; 44: 38–43.

21. Fukamizo T., Brzezinski R., (1997) Chitosanase from Streptomyces sp. strain N174: a comparative review of its structure and function. *Biochemistry and Cell Biology*; 75:687–696.

22. Yin H., Du Y., and Zhang J., (2009) Low molecular weight and oligomeric chitosans and their bioactivities. *Current Topics in Medicinal Chemistry*; 9:1546–1559.

23. Raghavendra V.K., Biswanath S.A., (2008) Evaluation of pH-sensitivity and drug release characteristics of (Polyacrylamide-grafted-xanthan)-carboxymethylcellulose pH-sensitive IPN hydrogel beads. *Drug Dev. Ind. Pharm*. 34 (12), 1406-1414.

24. Zhang J.P., Wang Q., Wang AQ., (2007) Synthesis and characterization of chitosan-g-poly(acrylic acid)/attapulgite superabsorbent composites. *Carbohyd. Polym.* 68: 367–374.

25. Huixia S.H., Wang W., Wang A., (2010) Controlled release of ofloxacin from chitosan- montmorillonite hydrogel. *Appl. Clay Sci*. 50:112.

26. Hori K., Sotozono C., Hamuro J., Yamasaki K., Kimura Y., Ozeki M., Tabata Y., and Kinoshita S., (2007) Controlled-release of epidermal growth factor from cationized hydrogel enhances corneal epithelial wound healing. *J. Control. Rel.* 118: 169

27. De Angelis, Capitani D., Segre A., Crescenzi V., (2001) Water in Hydrogels: An NMR study of water/polymer interactions in lightly cross-linked chitosan networks. *Polymer Preparation*. 42, 45-46.

28. Sannino, A., Esposito, A., Nicolais, L., Del Nobile, M.A., Giovane, A., Balestrieri C., Esposito R., Agresti M., (2000) Cellulose-based hydrogels as body water retainers. *J. Mater. Sci. - Mater. Med*. 11 (4), 247-253

29. Sannino, A., Mensitieri, G., Nicolais, L. (2004) Water and synthetic urine sorption capacity of cellulose-based hydrogels under a compressive stress field. *J. Appl. Polym. Sci.* 91 (6), 3791-3796.

30. Sannino, A., Esposito, A., De Rosa, A., Cozzolino, A., Ambrosio, L., Nicolais, L., (2003) Biomedical application of a superabsorbent hydrogel for body water elimination in the treatment of edemas. *J. Biomed. Mater. Res.* 67(3), 1016-1024

31. Superabsorbent hydrogels, (2006). Website of the leading Iranian manufacturer of superabsorbent polymers *Iran Polymer Society*, Tehran, 2-4,; Rahab Resin Co., Ltd.;

32. Ichikawa T., Nakajima T., (1996) Super absorptive Polymers (from natural polysaccharides and polypeptides), *Polymeric Materials Encyclopedia*, Salamone (Ed), CRC, Boca Raton (Florida), 8051-8059.

33. Buchholz F.L., Graham A.T., (1998) Modern Superabsorbent Polymer Technology, Wiley-VCH, New York, Ch 1-7.

34. Brannon P.L., Harland R.S., (1990) Absorbent Polymer Technology, *Elsevier*, Amsterdam, Ch 1-4.

35. Fereidoon S., Janak K.V.A., Jeon Y.J., (1999) Food applications of chitin and chitosans, *Trends in Food Science & Technology*, 10, No. 2, 37.

36. Banat I.M., Nigam P., Singh D., Marchant R., (1996) Microbial decolorization of textile-dye-containing effluents-a review. *Bioresour Technol*. 58:217–27.

37. Forgacs E., Cserhati T., Oros G., (2004) Removal of synthetic dyes from wastewaters-a review. *Environ Int*; 30:953–71.

38. Yin H., Du Y., and Zhang J., (2009) Low molecular weight and oligomeric chitosans and their bioactivities. *Current Topics in Medicinal Chemistry*; 9:1546–1559.

39. Sumiyoshi M., Kimura Y., (2006) Low molecular weight chitosan inhibits obesity induced by feeding a high-fat diet long-term in mice. *Journal of Pharmacy and Pharmacology*; 58:201–207.

40. Mourya V.K., Nazma, N., (2008). Chitosan-Modifications and Applications: Opportunities Galore. *Reactive & Functional Polymers,* 68, 1013-1051.

41. Crini G., Badot P.M., (2008). Application of Chitosan, Natural Amino polysaccharide, for Dye Removal from Aqueous Solutions by Adsorption Processes Using Batch Studies-A Review of Recent Literature. *Prog Polym Sci,* 33, 399-447.

42. Kawaguchi H., (2000) Functional polymer microspheres. *Progress in Polymer Science* 25(8), 1171-1210

43. Lee S.J., Kim S.S., Lee, Y.M. (2000) Interpenetrating polymer network hydrogels based on poly (ethylene glycol) macromer and chitosan. *Carbohyd. Polym.* 41:197–205.

44. American Dye Manufacturers Institute, Dyes and the Environment: Reports on Selected Dyes and Their Effects, vol. 2, New York, 1974.

45. Chiou M.S., Ho P., Ho Y., Li H.Y., (2004) Adsorption of anionic dyes in acid solutions using chemically cross-linked chitosan beads. *Dyes Pigm.* 60: 69–8

46. Blackburn S.R, (2004) Natural polysaccharides and their interactions with dye molecules: applications in effluent treatment. *Environ. Sci. Technol.* 38: 4905–490.

47. Helder L., Valfredo T.F, (2007) Chitosan modified with Reactive Blue 2 dye on adsorption equilibrium of Cu (II) and Ni (II) ions. *Reac. and Funct. Polym.* 67:1052-1060

48. Ollgaard H., Frost L., Gastler J., (1999) survey of azo-colorants on Denmark: Milgo, project 509. *Danish environmental agency.*

49. Juang R.S., Tseng R.L., Lee S.H., (1997) adsorption removal of Cu (II) using chitosan from a simulated rinse solution containing chelating agent. *Water Res.* 33:2403-2409

50. Maresh G., Clausen T., Lang G., (1989) Chitin and chitosan. *Elserv. Appl. Scien.* 389

51. Jiang X., Cai. K., Jing Z., (2011) synthesis of a novel water-soluble chitosan derivative for flocculated decolorization. *J. Hazard. Mater.* 185:1482-1488.

52. Wu F.C., Tseng R.L., Huang S.C., Juang R.S., (2009) Characteristics of pseudo-second-order kinetic model for liquid-phase adsorption: a mini-review, *Chem. Eng. J.*151: 1–9

53. Skoog, D.A., Holler, F.J., Nieman, T.A.,(1998). Principles of Instrumental Analysis, 5th ed. Saunders College Publishing, Philadelphia, USA, p. 303

54. Chen J., Park K., (2000) Synthesis of fast-swelling, super porous sucrose hydrogels. *Carbohydrate polymers.* 41:259-268

55. Ferreira L., Vidal M.M., Geraldes C.F, Gil M.H., (2000) Preparation and characterization of gels based on sucrose modified with glycidyl methacrylate. *Carbohydrate polymers.* 41:15-24

56. Jia Z., Shen D., Xu W., (2001) Synthesis and antibacterial activities of quaternary ammonium salt of chitosan, *Carbohydr. Res.* 1:1–6.

57. Domard A., Rinaudo M., (1986) Polyelectrolyte complexes. *Int. J. Biol. Macromol.* 8:105–119.